Creation of Tri-Planar Incisions in Vitrectomy

An Explorative Design-Study into Trocar Insertion Mechanisms

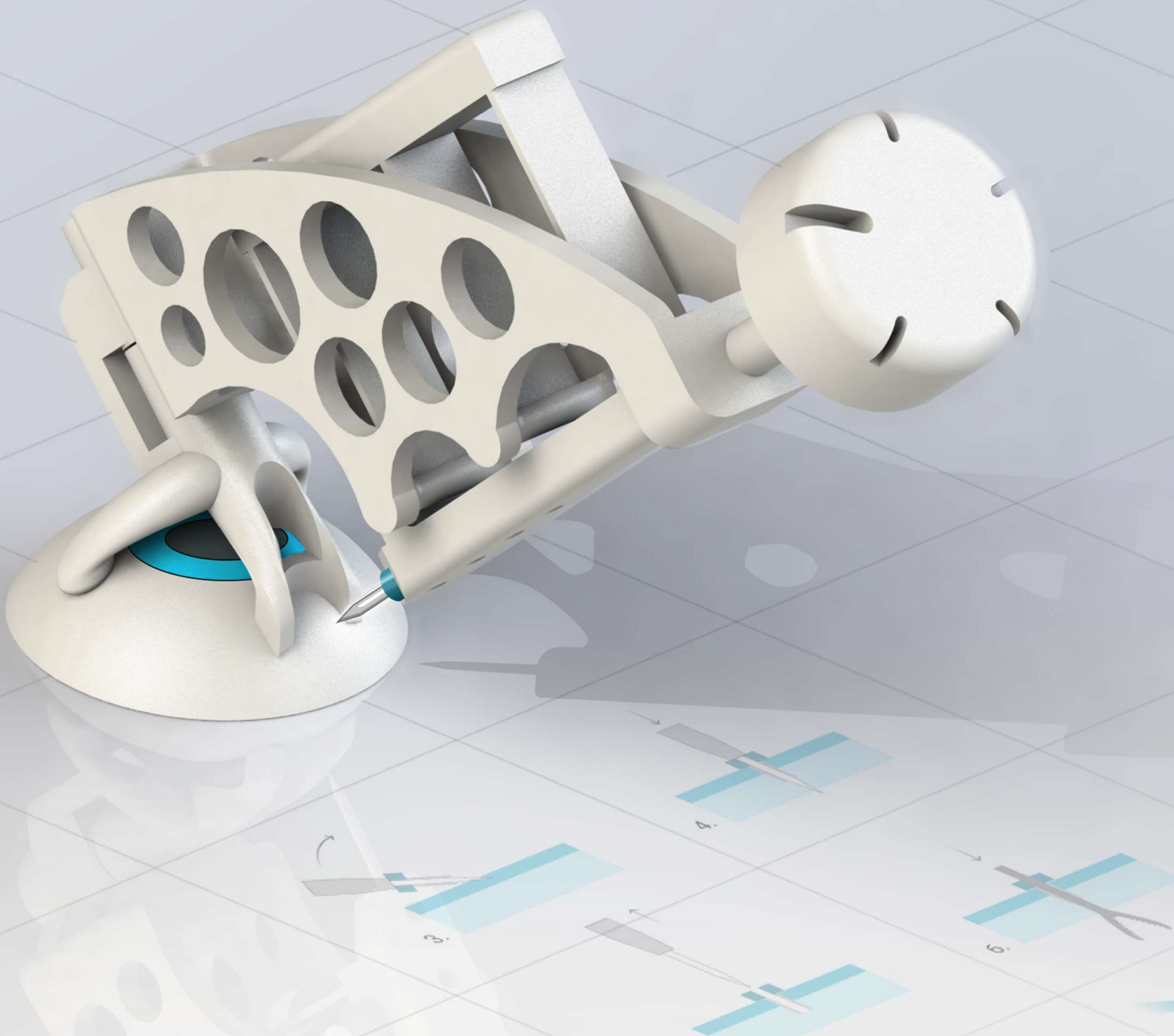

Berend B. Koot

TU Delft

Creation of Tri-Planar Incisions in Vitrectomy

An Explorative Design-Study into Trocar Insertion Mechanisms

By

Berend B. Koot
Student number: 4379489

In partial fulfillment of the requirements for the degree of

Master of Science
In Mechanical Engineering

At the Delft University of Technology

June 30th, 2021

Main supervisor: prof. dr. ir. P. Breedveld	TU Delft
Second supervisor: prof. dr. J. Dankelman	TU Delft
Daily supervisor: ir. K. Lussenburg	TU Delft

Abstract

Background: In vitrectomy, a type of eye surgery, surgery instruments must pass through an incision in the sclera. The architecture of the incision is of great importance to the closure of the wound after the procedure and through that the risk for complications like hypotony and endophthalmitis. Current studies suggest that tri-planar incisions provide better sealing, however for a surgeon it is challenging to produce the desired architecture easily and consistently. The objective of this study is to: "*Design and verify a new, reliable and easy to use method to create tri-planar incisions for scleral cannulas to limit leakage after extraction of the cannula.*"
Method: Analysis of the factors affecting the tri-planar incision method in terms of reliability and ease of use was performed, leading to a set of design requirements. Based on the requirements, different incision methods were explored and compared. The selected method was transformed into a functional prototype, which was subsequently evaluated on consistency and leakage. The evaluation was done by insertion on silicone sheet, eye phantoms and ex-vivo porcine eyes. The tri-planar incision was compared in leakage to straight and oblique incisions, two other common type of architectures.
Results: The method performed using a designed device was able to create the desired tri-planar consistently. These incisions provided a better seal than a straight incision. However, for tri-planar compared to an oblique incision the test was inconclusive and further research is needed to distinguish between the two.
Conclusion: As tri-planar incisions can now consistently be made with the use of the new method, further research can be performed to link the number and type of complications, like hypotony and endophthalmitis, to the incision statistics.

Table of Contents

1 Introduction

1.1 Creating a Passage

The human eye is a very delicate organ and has a huge influence on how humans function. Eyesight gives people the window through which they view the world. The eye is very sensitive and around 70% of sensory receptors present in the human body are in the eye and nearly half of cerebral cortex is involved in the processing of visual stimuli [2]. It is therefore not surprising that in an online survey held in the United States, respondents across all ethnic and racial groups described loss of eyesight as the worst ailment that could happen to them, relative to losing memory, speech, hearing, or a limb [3]. Hence, it can be quite problematic when an eye is not functioning the way it should.

In some cases, a surgical procedure called a vitrectomy is necessary to regain vision or prevent further damage. In this procedure, the fluid inside the eye is removed and replaced with a different fluid. This is necessary, for instance, when the fluid has clouded or in case of a retinal detachment, when the retina detaches from the posterior part of the eye. To limit the risk of compromising vision, it is paramount that the delicate eye tissue is perturbed minimally during the surgical procedure. Minimally invasive surgery techniques have been developed in which the surgery on deeper lying structures is performed through a small opening, minimizing collateral damage. An image of the eye during a minimally invasive surgery can be seen in Figure 1.

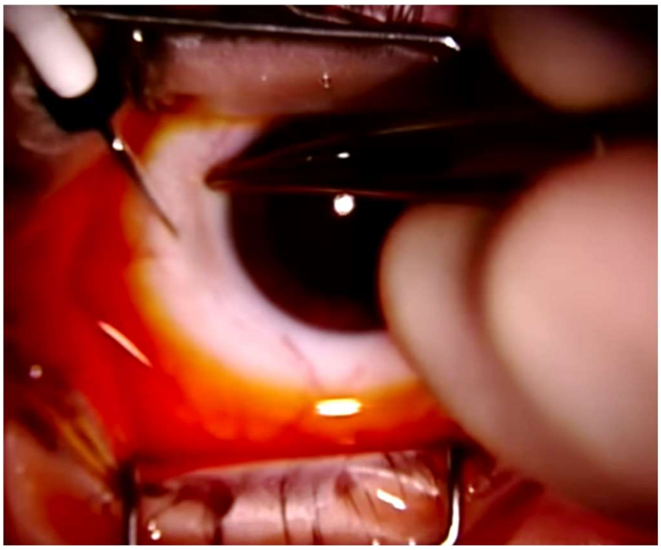

Figure 1: Trocar insertion performed by dr. Van Etten [4].

In the conditions described above, surgery instruments have to pass through a small hole in the tough white sclera to be able to reach the inside of the eye. To enable the passage of instruments whilst making minimal damage, a tool called a trocar is used. The trocar knife clears a passage through the sclera and on retraction places a cannula, a small tube section that holds the wound open during the surgery. The path the trocar knife takes is of great importance to the closure of the wound. The wound architecture, i.e., the specific geometry of the wound, should be designed in such a way that it seals itself under the intraocular pressure (IOP) after extraction of the cannula. Self-sealing behavior without sutures is called a sutureless incision.

1.2 Problem Definition

Currently, surgeons use an oblique incision architecture, in which the trocar knife does not enter perpendicular to the surface, but under an angle. Even though an oblique architecture provides an acceptable closure, complications like hypotony and endophthalmitis still occur, with rates of 3.3-11% and 0.2% respectively [5, 6]. It is expected that there are possibilities to reduce complications through better wound sealing. Current studies suggest that tri-planar incisions provide better sealing, however for a surgeon, it is challenging to produce the desired architecture easily and consistently [6-9].

In medicine, there is a wish for tri-planar incisions to prevent wound leakage after cannula placement. However, this incision method cannot be verified as currently there is no tool available for reproducible and easy evaluation of tri-planar incision architectures. Current clinical trials of alternative architectures therefore show a large spread in results, have small group sizes and have a large number of uncontrolled variables. Further exploration and verification of the method is required, this thesis will aim to fill this gap.

1.3 Research Objective

The wish for the innovation of a clinical instrument for cannula placement to reduce complications through better wound sealing, has led to the research objective: **"Design and verify a new, reliable and easy to use method to create tri-planar incisions for scleral cannulas to limit leakage after extraction of the cannula."**

This explorative study will be performed in a process covering the analysis of the factors affecting the tri-planar incision method in terms of reliability and ease of use, leading to a set of design requirements, a translation of the requirements into a functional prototype design, and a validation of the method through experimentation. If the method is successful, it should be possible to further develop the proposed mechanism into a surgical product. To reach the research objective, the following research questions will be answered:

- What are the factors of influence in vitrectomy?
- What are the requirements for new method?
- What are possible solutions for a new method?

- Does the method and resulting tool meet the requirements?

The answers to these questions will be given in this report and summarized in the conclusion.

1.4 Layout of this Report

This report will describe all steps taken in this thesis project, show the insight into this mechanism and argumentation of the design choices. Each Chapter describes one phase of the process. The second Chapter starts with an analysis of the circumstances in the operation room and the wishes of the surgeon regarding a new tool, leading to the factors of influence in vitrectomy. In the third Chapter, the analysis is translated into a set of requirements that can be used for evaluation of possible solutions and in the creation of a conceptual design. In the fourth Chapter, the conceptual design is dimensioned to a functional prototype. In the fifth Chapter, the prototype is used to validate whether the requirements and the wishes of the surgeons have been met, leading to a discussion of the design and a conclusion.

2 Analysis of Vitrectomy

2.1 Analysis Objective

The medical field is quite different than what a mechanical engineer would normally encounter. The objective of the analysis is to gather background knowledge and lay the groundwork for the constraints and requirement in a mechanical design. The chapter starts with some theory of both the anatomy of the eye and the current surgical procedure and continues with an analysis of the factors that are of influence in creating well sealing incisions.

2.2 Anatomy of the Eye

2.2.1 Overview

To understand the method of surgery, a short introduction to the anatomical structure of the eye is necessary. Going from the outer layers to the inner layers of the eye, the fibrous, vascular and inner layer are found encapsulating the inner chambers and fluids[2]. The functions of these layers are described below. The anatomy is also visually represented in Figure 2.

2.2.2 Fibrous Layer

The layer on the outermost shell of the eye consists of a dense fibrous layer of connective tissue without any blood vessels. Its purpose is giving structure to the eye and maintaining the intraocular pressure. It consists of two distinct parts, the sclera and the cornea. The **sclera** is the posterior portion and makes up the largest part of the outside of the eye and is visible on the outside as the 'white of the eye". It protects the eye and functions as

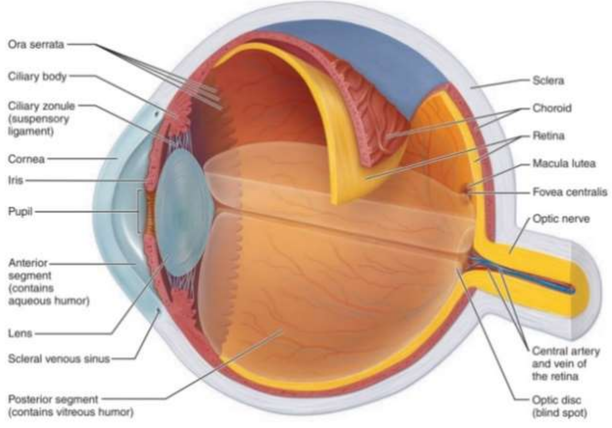

Figure 2: Schematic anatomy of the eye [2].

an anchoring site for the muscles that turn the eye. On the back there is a single hole where the nerves from the retina exit called the optic disk. This location is also called the blind spot due to a lack of vision. The **cornea** is on the anterior side of the eye and the modified fibrous layer act as a window to let light enter the eye. Both the sclera and the cornea do not possess any blood vessels.

2.2.3 Vascular Layer

The middle layer of the eye is called the vascular layer. It consists of three parts with different functions and morphology, the choroid, ciliary body and iris. The **choroid** is a well vesiculated layer covering the largest portion of the inside of the eye, supplying the other layers with blood. Pigment in this layer gives it a dark brown color preventing unwanted reflections within the eye that would distort vision. More anterior of the choroid its thickness increases forming the **ciliary body**, a thick ring enclosing the lens. Muscles in this ring allow for reshaping the lens, enabling a person to change the focal length of the eye. The **iris** is the colored part of the eye that can be seen from the front. It has a hole in the middle called the pupil that can be varied in diameter to control the amount of light that enters the eye.

2.2.4 Inner Layer

The innermost layer is called the **retina** and developed from an extension of the brain. It contains the sensing cells, called pigment cells on the outside and a thin network of neurons on the inside. These cells detect and convey the visual information that enters the eye. Even though the cells are very close together, they are not fused and may get detached. The densest packing of pigment cells is found on the **macula**, the place where the lens of the eye focuses and which is most important for vision. The retina covers most of the inside of the eye except for the last few millimeters on the anterior side. This leaves a small band between the ciliary body and retina with less structures, which is called the **pars**

plana. The lack of vital structures creates a location in which the eye can be punctured with limited consequences which is crucial in surgeries in the posterior chamber. The incision that is made for these has to be positioned in this region, marked in Figure 3, to prevent complications.

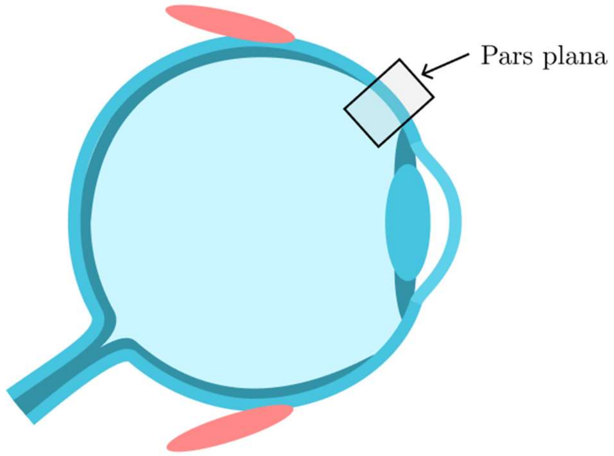

Figure 3: Location of the pars plana marked with a box, at this location instruments can be inserted.

2.2.5 Internal Chambers and Fluids

The structures above effectively form two different chambers, the anterior and posterior chamber with a **lens** in between, a convex transparent structure able to focus light. The **anterior chamber** is located anterior of the lens and contains aqueous humor, a watery substance similar to blood plasma. It forms and drains continually, providing oxygen and nutrients to the cells in the cornea and lens. In addition, it provides some pressure from within the eye to retain its shape. The **posterior chamber** is filled with a clear gel called vitreous humor containing a lot of water. It is clear to allow the light to pass, but also provides some structure to the inside of the eye. Unlike the aqueous humor it does not drain.

2.3 Indications for Vitrectomy

There a several indications for a vitrectomy, a surgical step in which the vitreous humor, often referred to as the vitreous, is removed, like detachment of the retina and problems with clouding of the vitreous humor. Degeneration of the eye during life is an important factor in these conditions. In the case of a young eye the vitreous humor will support the more outward structures of the eye, keeping the retina in place. With degeneration over time, the vitreous humor of the eye may lose some of its clear gel-like substance and will start shrinking [5]. On retraction during shrinking, the volume will fill with a more neutral fluid, which does not affect vision negatively. However, at some spots, the fibers in the gel might form a stronger bond with the retina and start pulling on it, resulting in tension on the retina eventually detaching it from the outer layers. In a worst-case scenario such a detachment could lead to a macular hole, a break in the retina at the macula, greatly impairing vision. The degeneration might also cause clumping of the proteins in the vitreous humor causing it to become cloudy. To prevent propagation of the detachment and allow the retina to heal or resolve the impaired vision due to clouding, it is necessary to do a vitrectomy.

2.4 Current Surgical Procedure

To reach the vitreous humor, a passage must be made through the sclera, which is done using a trocar-cannula system. The step of going through the sclera is called a sclerotomy. Two techniques have been described for wound construction, each requiring a slightly different set of instruments. One method is a two-step incision sclerotomy. The first step involves using a stiletto blade to create the initial passage, which is followed by the placement of a cannula, a tubular part that holds open the incision for the insertion of instruments during surgery, over a blunt inserter [10-12]. The method produces wounds that seal well and therefore often do not need suturing. However, it has the disadvantage of needing more instruments during the procedure and the difficulty of finding the incision when placing the cannula is higher [5]. The more common approach is the single step method uses a trocar cannula set. The set consist of a handle with a sharp tip called the trocar knife, the cannula is placed. An example of such a system sold by DORC (*Dutch Ophthalmic Research Center, Zuidland, The Netherlands*) is depicted in Figure 4. In this model, the handle also has a scleral marker on the back to measure the position on the pars plana and to find the right location for insertion. The one-step method combines the puncturing and placement in the same device. The sharp tip of the trocar punctures a small hole through the sclera, providing access to the inside of the eye. This cannula enters the sclera together with the trocar and

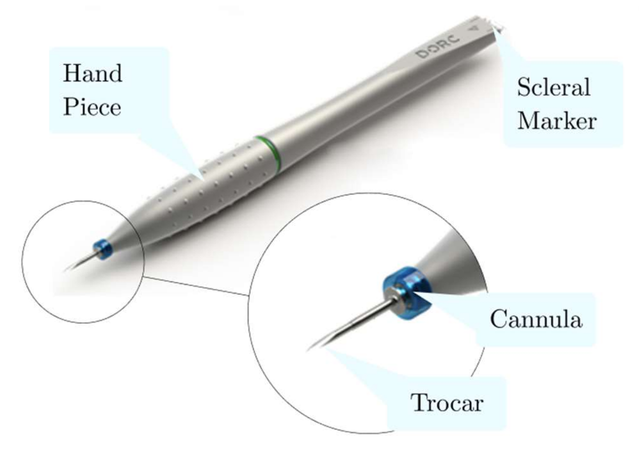

Figure 4: Trocar system manufactured by DORC [1].

supports the passage once the handle is removed. Some cannula may also feature a valve to prevent vitreous fluid from leaking out when no surgical apparatus is present to seal the hole [5].
Several other manufacturers offer systems similar to the one made by DORC [13], having slight differences in blade and cannula geometries. Although there are slight performance differences between the different geometries [14], the use of the device is the same. As the single step method and the combined trocar-cannula set is dominant due to its ease of use, this report will focus on this method.

Most of the surgery is done on a visual basis, using an operating microscope to aid the surgeon. With a foot pedal, the surgeon can control the zoom magnification, focusing and the X-Y movement, A beam splitter is used for the surgical assistant [5]. During the start of the surgery when the trocars are placed, the microscope has a clearance of 10-20 cm from the head, depending on the microscope model. During the interventions further in the eye an additional lens can be folded out, called a 'fundus viewing system", positioned very close to the eye (personal communication DORC, 27 January 2021). During the surgery, the fluid pressure is kept constant through a highly regulated inflow of fluid though one of the cannulas connected to a pumping device. For the removal of the bulk vitreous, a vitreous cutter is used, which is a tube section with a powered cutter on the end, cuts the vitreous and transports it out of the eye. It enters the eye through another cannula. Inside the eye, the surgeon also uses micro-forceps small enough to fit through the cannula for manipulation. These can be used to peel of the last remnants of the vitreous humor. Some light is introduced from the outside, however, when this is insufficient, a fiberoptic light can be introduced through a cannula.

Based on a recording of a macular hole repair by dr. Van Etten [4], also depicted in Figure 1, and an interview with dr. Crama the following steps were identified.

1. The sclera is marked with the back side of the device to determine the correct position on the pars plana (square box in Figure 3). This creates a small dimple that acts as a reference.
2. The trocar knife is inserted under an angle of around 30°, this angle is chosen to be as flat as possible whilst the trocar should still be able to penetrate the sclera. To prevent rotation of the eye, it is held in place with forceps. These should be in line with the sclerotomy site and the direction of insertion to prevent torque.
3. When the trocar is partially in the sclera it is rotated into the perpendicular position. This will create a two planar incision; other surgeons go all the way through before rotating.
4. Next the trocar is inserted all the way, to the point where the rim of the cannula prevents further insertion.
5. The trocar knife is extracted, but the cannula remains. Steps 1-5 are then repeated for the desired number of cannulas. For most surgeries at least three passages are necessary, one for light, one for apparatus and the last on to maintain a constant intraocular pressure.
6. The surgery is now performed using the created passages. Depending on the type of repair the surgeon inserts a different set of tools through the cannulas.
7. When the surgery is over the cannulas are extracted and disposed.
8. The wound is massaged shut with a cotton applicator.

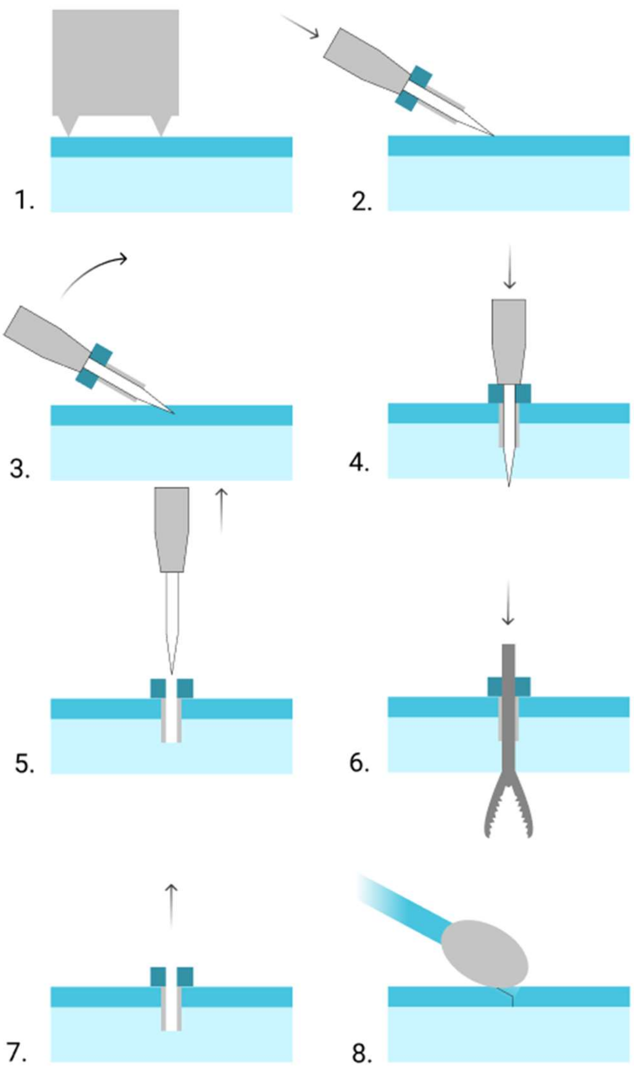

Figure 5: Steps in the insertion of a trocar canula system. For numbering and more information see text.

Depending on the surgeon's preference there is several optional steps that can be added after the surgery. Firstly, the insertion is done under an angle to enable a proper closure of the incision post operation; the intraocular pressure will close the gap. For smaller gauge instruments this is often enough to keep the incision closed, for larger gauge instruments or in case of improper sealing a suture might be necessary. Secondly, after the surgery the surgeon has the option to leave a tamponade, often a bubble of gas or a silicone oil. The choice between the different tamponades is made on clinical experience [5], however merely looking at the sealing of the wound gas tamponades seam to seal better than fluid [15]. Thirdly, after surgery an optical coherence tomograph (OCT) can be used. This imaging device provides a real time image of the microstructure in two dimensions, similar to the image of an echo. The images created using this technique provide a very clear image if the pathology was resolved and assist the surgeon in determining the prognosis of recovery [5].

2.5 Mechanical Analysis of a Scleral Element

2.5.1 Forces on the sclera

To gain insight in the mechanics of insertion and sealing, it necessary to look at the forces on the sclera during and after insertion. The parameters that play an important roll here are the biomechanical properties, the normal stress state due to ocular pressure forces and the forces added due to the insertion of the trocar.

2.5.2 Biomechanical Properties

The sclera is a relatively hard outer shell of the eye, giving it most of its shape. The material properties as mostly determined by its fibers. The fibers are oriented in all directions within the scleral plane, but not perpendicular, making it highly anisotropic [16-21]. The elasticity is highly nonlinear [17, 19, 22] and is measured to be around 26MPa in cadaveric eyes [18]. Computer modeling has been attempted, but remains difficult due to the non-linear nature of the sclera [23]. Very limited research has been done on the deformations of the sclera on insertion in general and especially on oblique or triplanar insertions, or the behavior of the wound post-surgery.

The biomechanical properties have some variance over age. Younger eyes have a more flexible sclera and therefore are more likely to have improper wound apposition [6, 20, 22]. This might in some cases lead to insufficient sealing, even when an oblique incision is performed. However, surgery in younger eyes is less common and problems related to improper sealing due to the more flexible sclera are therefore rarer.

2.5.3 Pressure Forces

The forces that act on the sclera as a result of the normal IOP, have an effect on the wound. The sclera can be simplified as a thin-walled pressure vessel, as its thickness of around 0.5mm is a lot smaller than its radius of 12mm. [2] As a rule of thumb, if the thickness is less than $1/10^{th}$ of the radius the stress will vary less than 5% over the thickness and the thin-walled assumption is acceptable. [24, 25] An element of such a sphere is depicted Figure 6.

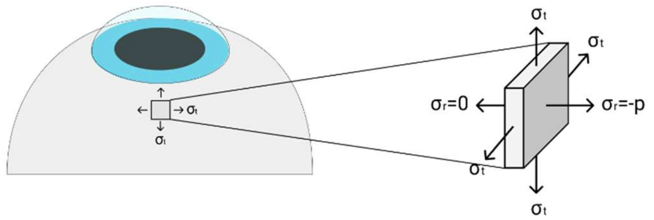

Figure 6: element of thin walled sphere representing the eye bases on [24] , where σ_t is the tangential stress, σ_r is the radial stress and p is the intraocular pressure.

Due to the rotational symmetry the tangential stress is equal independent of the direction of the element and there will be no shear stresses on an element on the sphere. The forces on the element on a thin-walled sphere have been worked out by *Kelly et al* [24]. From the force balance of one-half of the sphere is, it can be deducted that the shear stress should be Equation (1), where p is the pressure, r is the radius of the eye and t is the wall thickness.

$$\sigma_t = \frac{pr}{2t} \tag{1}$$

$$\sigma_r = -\mathrm{p} \rightarrow \sigma_r = 0 \tag{2}$$

The radial stress of the material is the internal pressure of the vessel and decreases to atmospheric, where it is taken as zero, this is depicted in Equation (2) with an arrow. Both [24, 25] neglect the internal pressure as it would be 10 times as small than the radial stress. This is admissible when looking at the general stress state of the material. Even though the radial stress is insignificant to the general stress state of the material it still has an important influence. The pressure gradient along the wall is a driving force for fluids from within the eye to move out. In addition, the pressure gradient creates an architecture that is self-sealing.

$$\begin{bmatrix} \varepsilon_t \\ \varepsilon_t \\ \varepsilon_r \end{bmatrix} = \begin{bmatrix} 1/E & -\nu/E & -\nu/E \\ -\nu/E & 1/E & -\nu/E \\ -\nu/E & -\nu/E & 1/E \end{bmatrix} \begin{bmatrix} \sigma_t \\ \sigma_t \\ \sigma_r \end{bmatrix} = \frac{1}{E}\frac{pr}{2t} \begin{bmatrix} 1-\nu \\ 1-\nu \\ -2\nu \end{bmatrix} \tag{3}$$

The stresses on the wall due to the pressure cause strains in the material, one strain for each direction of stress, two planar and a single radial strain. Using Hooke's law these can be calculated using Equation (3), where E is the elasticity modulus of the material and v is the Poisson's ratio. When the pressure increases the wall will stretch in the planar directions, increasing the circumference of the sphere. In the radial direction the sphere will thin, as can be seen by the negative sign in the vector.

This analysis makes it clear why the oblique incisions perform better in sealing than straight incisions. The tangential force on the sclera due to pressure stretches the hole and makes is larger, whereas the oblique path will be pressed close due to the internal pressure. The more oblique the incision, the larger the projection of the force on the surface of the incision and therefore better sealing.

2.5.4 Trocar Forces

When introducing a trocar blade the sclera will resist insertion. The blade will experience three types of force, an axial force due to puncturing the sclera, cutting force of the blade and a friction force once it has passed the sclera. Factors that are of importance for the insertion force are the size of the trocar, velocity, geometry, vibration, and rotation [26-29]. A confirmation of these factors can be found by looking at nature. A search yields a group of animals that have developed and optimized the same factors [30-32]. There is a distinction between biological and artificial tissue with respect to velocity. There is a reduction in force with higher velocity in biological material, but not in artificial material. This might be due to thixotropy of biological material, where the silicone based artificial material respond more viscous. [27]

Limited information is present in literature about the insertion force of an in-vivo sclera. Table 1 shows the insertion force for different trocar sizes, from this a best estimate must be made for the insertion force of a trocar in-vivo. To add this the values are plotted in Figure 7. As an assumption the mean force of around 1,5N for the insertion of a 23G trocar was used as the force that is currently applied in surgery until more research is done [14, 33]. For a 25G trocar this value would be lower, interpolating between the reported values of 23G and 27G would yield a force of around 1N.

Table 1: reported trocar force in different papers.

Force	Size	Experiment	Paper
0.70-1.00N	18G	Ex-vivo sclera	[32]
0.52-2.83N	23G	Artificial sclera	[11]
0.54-0.68N	27G	Ex-vivo sclera	[34]
0.19-0.27N	30G	Ex-vivo sclera	[34]
0.27-0.31N	31G	Ex-vivo sclera	[34]

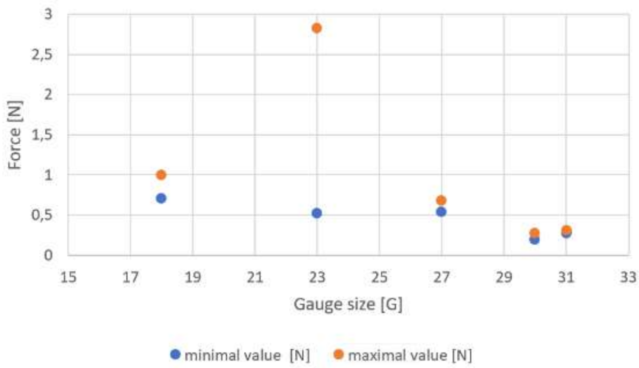

Figure 7: Maximum and minimum trocar insertion force plotted against gauge size.

2.6 Factors of Influence on Surgical Tooling

2.6.1 Gauge Size

The size of the incision is determined by the gauge of the tools. The gauge is a measurement of size and the higher the gauge number, the smaller the size of the tool and required hole. Small gauge surgery is becoming increasingly popular as patients experience much less post-operative discomfort and visual recovery is faster as well [35]. Due to the smaller size of a 23G (0.6mm) or 25G (0.5mm) as opposed to 20G (0.9mm), often no sutures are necessary if the wounds are self-sealing. [35]. The main disadvantage is the smaller instruments lose some stiffness and require higher pressure to exchange fluids. [5] The 23G size is currently the most common, however the trend is a reduction of size to 25G instruments.

2.6.2 Incision Style

Incision Variations

Interviews with the eye surgeons, Peter van Etten, Niels Crama and Sander Keijser pointed out that incision architecture is of importance to prevent leakage through the wound and minimize the associated higher risk for Endophthalmitis and Hypotony. The interviews are summarized in Appendix A. Three different

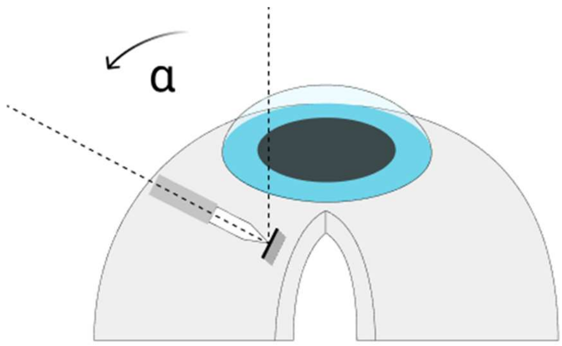

Figure 8: Incision angle (α) of the trocar knife (dotted line through the grey handle) with respect to the normal of the scleral plane (vertical dotted line).

architectures have been identified, single plane oblique, bi-planar and tri-planar incisions. Each different incision is made through a variation of angle with respect to the scleral plane (α) and the insertion depth, depicted in Figure 8.

Oblique Incision

Over the last years there has been some development in the geometry of the incision. In the past sutureless vitrectomy was performed using a perpendicular entry with respect to the sclera, where α is zero. The perpendicular incisions were altered to more oblique incisions, where the trocar is inserted in the sclera under and larger angle α, as these incisions provided a better sealing wound. [8, 15, 36] First oblique self-sealing sclerotomies for pars plana vitrectomies were first described by *Chen et al* [37] and developed further over the years by other researchers and have become the standard method. The theory is that the IOP closes the wound and prevents exchange of fluid between the inside and outside of the eye. In eyes with good wound apposition, the IOP remained higher after surgery, as opposed to those with loss of wound apposition, where IOP dropped [38]. In other words, wounds that have more contact of the cut surface close better. The architectural features of gaping, misalignment, and great variation in incision angle reduce the security of sutureless sclerotomy directly after the surgery. These features presumably predispose the patient to lower IOP and greater risk of wound leakage. [38] However, even though oblique incisions have improved the closure of the scleral wound significantly, Hypotony and Endophthalmitis still occur [6], with rates of 3.3-11% and 0.2% respectively. [5]

Bi-planar Incision

More elaborate incision architectures are also being tested, consisting of more than one plane. During the insertion the trocar knife is tilted to create a step. This method is used by dr. Crama and depicted in Figure 5. The idea is twofold, the incision path is longer, creating a longer path for germs to travel and secondly the incision can be oriented more in plane with the sclera, whilst still providing an acceptable angle for the instruments to pass. However, the bi-planar approach is not without critique as it has been proven to be very difficult for surgeons to perform successfully on a consistent basis [35]. As the sclera is only around half a millimeter, there is not much room for margin. The deformations in the eye during the surgery are quite large as can be seen in a video recording of dr. Van Etten. [4] , making it more difficult to find a fixed reference. In addition, the peak to peak physiological hand tremor, the amount of involuntary movement the surgeon makes when trying to hold his instrument completely still, already results in a significant variation compared to the scale of the scleral thickness. [39] It is therefore not surprising that only 55% of the incisions that were made during their experiment showed a two-plane structure when analyzed using optical coherence tomography (OCT), an imaging technique similar to an echo except using light instead of sound waves [8]. Bi-planar scleral incisions may be more difficult to reproduce consistently and if done incorrectly produce more internal wound disruption upon turning. This fraying is detrimental to the effective path length and thus compromises the effectiveness of the seal [8, 16].

Tri-planar Incision

Tri-planar incisions are commonly used in cataract surgeries. In a cataract the fibers create the optical properties of the lens may start to clump, creating a milk white hue over the entire image. [2] It can be resolved by removing the lens and replacing it with an artificial lens. In a cataract surgery the anterior chamber of the eye is accessed through the cornea. The incision architecture has been studied in more detail for cataract surgery than for vitrectomy. Bi-planar and oblique incisions constructed at smaller angles to the surface provided a better seal when faced with increased intra ocular pressure. [40, 41] The tri-planar incisions could further minimize leaking, however just like the bi-planar incision they are difficult to construct. One study showed that when aiming for a tri-planar incision, the resulting wound will only be thri-planer in 32% of the eyes. [7] Although these studies were related to corneal incisions, it is reasonable to expect sutureless scleral incisions to behave in the same manner based on the geometry of the incision. [8] The shape of the incision is depicted in Figure 9.

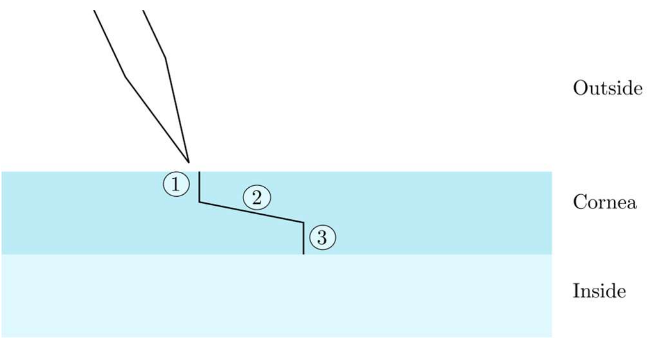

Figure 9: Multi planar incision by Spandau et al [9]. The incision is depicted using the black line. The numbers mark the three planes.

The tri-planar approach was successfully copied from cataract surgery to a vitrectomy [6]. The incision was made using a small stiletto knife and the cannula was inserted using a blunt inserter. In a series of 45 eyes operated using this approach no cases of hypotony were reported. However, the method has not gained a lot of ground, possibly due to being more complicated and time consuming to perform. The surgeon used a two-step approach were the incision and placing of the cannula are performed in separate steps, taking more time. As opposed to incisions in the sclera, multi-planar incisions during cataract surgery are simpler as the cornea in which the surgery is performed is clear. dr. Crama suggested that the improved feedback on depth in the clear medium of the cornea makes construction of a more complex architecture more successful.

In conclusion, single plane oblique incisions are the standard, as multiplanar incisions are difficult to construct by a surgeon, as the sclera is opaque, and the margins of error are low and when constructed incorrectly have a negative effect on the effectiveness of the seal. Ideally, we would be combining the simplicity of a single plane approach with the performance of the three planar.

2.6.3 Direction of the Tunnel and Direction of the Incision

When creating an incision in the sclera there are two orientations that are of importance. The direction of tunnel of the trocar (β in Figure 10) and the direction of the incision (γ in Figure 11).

Using these two variables there are four possible combinations. In Figure 12, variations 1 and 3 are in plane with the sclera, as opposed to perpendicular and variations 2 and 3 the paths are in the concentric direction, as opposed to radial.

As opposed to the cornea, where the fibers are oriented in concentric circles, the fibers in the sclera form an irregular network in both the superficial and deep sclera. Originally it was assumed that it might be possible to separate fibers instead of cutting, creating a better sealing wound when cutting in the direction of the fibers [16]. However, irregular fiber orientation would consequently result in an indifference of direction of the tunnel on the success rate of the surgery. Choosing the direction there is another important factor to consider, which is the risk of hitting other structures. A radial path would increase the risk of puncturing the retina or lens and therefore the circumferential path, like 2 and 3, is preferred [5, 16].

The orientation of the incision with respect to the scleral plane is of greater importance. The incisions that were more in plane, therefor having a low value for γ (incision 1 and 3) provided a better seal [16]. In force analysis of the sclera, it became clear that this is likely due to a predominantly perpendicular force on the sclera. In addition, in the case of a perpendicular incision pathogens and fluids can travel across the width of the incision, decreasing the effective path length.

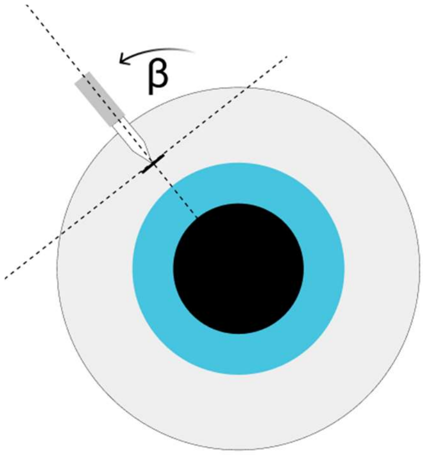

Figure 10: Direction of tunnel tangential to the eye (β). The angle is measured through the dotted lines through the dark gray handle to the tangential line through the limbus.

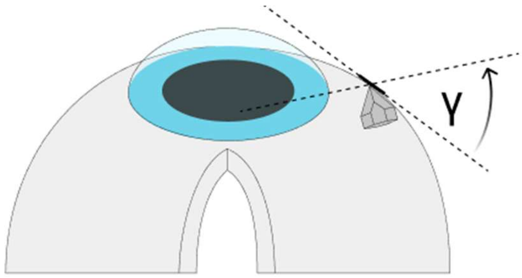

Figure 11: Direction of incision through rotation of the trocar blade. Angle (γ) between scleral plane and the cutting plane of the blade depicted with dotted lines.

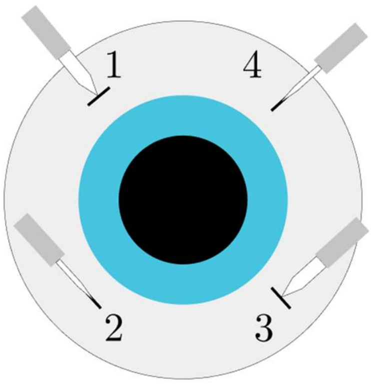

Figure 12: Possible combinations of incision directions when inserting a trocar in the eye [16] Black lines represent the incisions.

In conclusion, there is not a large difference in effectiveness of the seal between radial and circumferential paths, as long as no other structures are damaged. The direction of the blade is of importance and should be oriented in plane with sclera, in such a way that pressure will close the wound. Currently option 3 will have the best result, which was confirmed by the number of leaking sclerotomies [16].

2.6.4 Other factors to Consider

Length of Surgery

Time in the Operation Room (OR) is expensive and should be kept low to keep cost down. In a video by dr. Van Etten [4] the placement of three trocars took well under a minute. He responded in an interview that the total surgery typically takes around 45-60min for a macular hole repair, therefore the current insertion time of trocars is only a small part of the surgery. Time lost during extra steps with insertion of the trocar would not lead to saving time somewhere else. A new tool could save time if it does not need massaging to close the wound, however it is unlikely that a newly developed tool would achieve this. dr. Crama added that even though the consequences of leakage are high, the severe complications are still relatively rare. Due to this trade-off, a new approach should not take significantly longer than the current insertions of the trocars. A value below 30s would be acceptable during the explorative phase for experiments, however the system would have to be scalable to a faster mechanism.

Positioning Method

When asked, the surgeons stated in their interviews, found in Appendix A, that they would like to have full control where they place the incision. In case a mechanism would be better at making an incision in every eye, they would not mind losing some control over the incision architecture. There is some variation in the sclera from one person to another. In case the mechanism does not handle the variations, they would like to be able to compensate for that. The current positioning method using a measuring tool from the limbus seems sufficiently precise.

Single Use

There is competition between single use instruments that can be disposed of after surgery and reusable instruments that can be reused after sterilization. The current trocar knives are single use and so are many more recently developed surgical tools. Single use tools are often more expensive in use than reusable equipment. [42] However, the risk for complications decreases and the total cost can be compensated for [43]. In this design process the focus is on reducing complications, therefore single use is preferred.

Adjustability of Geometry

Not every patient is the same. At the pars plana the sclera is around 0.53mm with a standard deviation of +-0.07mm [44, 45], therefore surgeons must be able to compensate for a wide range thickness. Assuming the scleral thickness is spread like a normal distribution, the 95% confidence interval ranges between 0.39-0.67mm, as depicted in Figure 13. As the spread is relatively large, the geometry of the incision has to be adjusted to the individual thickness of the patient's sclera. In addition, the ability of adjusting the geometry would allow surgeons to gather more data about the effects of variations in geometry.

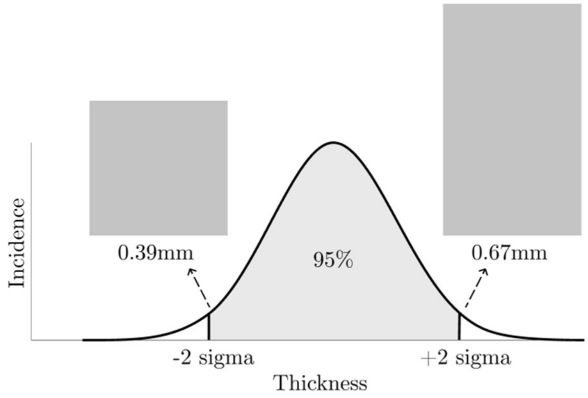

Figure 13: Distribution scleral thickness with the 95% interval shaded in grey. At the ends of the interval the thickness is depicted with a bar.

Intraocular Pressure

Currently the insertion of the trocar knife results in a sudden spike in intraocular pressure, limited applicability of the insertion method in certain conditions. One such condition can be an open eye trauma, where added pressure can lead to further tearing or insufficient counterpressure is present for insertion. Or in patients with glaucoma where the pressure already is high [28, 35, 46]. The pressure will rise from around 15 mmHg [47] up to 68mmHg [46], but may even be higher if measured using a higher time fidelity where it can reach 89mmHg [28]. However, for the standard vitrectomy this rise in pressure is clinically irrelevant, according to dr. Van Etten and dr. Crama. Other manipulations during the surgery likely cause even higher pressures and dr. van Etten never encountered it to be a problem. A summary of the interviews with the surgeons can be found in Appendix A.

3 Conceptual Design

3.1 Design Process

Design is an iterative process going back and forth between the design requirements and wishes, and the resulting concepts that have been generated. In this process there is a constant optimization of the different parameters of the design. In this chapter the design process will be described by the main components in envelops, the design requirements, orientations of design direction and argumentation, leading to the final conceptual design.

3.2 Design Requirements

3.2.1 Approach

The goal is to explore and verify a new, reliable, and easy to use method to create tri-planar incisions for scleral cannulas to limit leakage. To design an instrument that will verify this new method, requirements in the different categories were defined, with the addition of wishes that would aid the development of a future product. The basis for the requirements has been made in the previous chapter. In addition, a stakeholder analysis was performed, included in Appendix B. This project aims to be surgeon driven, solving a problem encountered by surgeons in the field and providing the tools to improve the outcomes for patients. The design requirements are divided in three different categories, functional, geometric, and ergonomic requirements. The design requirements in these three categories are summarized in

Table 2.

3.2.2 Functional Requirements

The main function of the tool is to create tri-planar incisions and increase the control over the insertion depth and angle. During the insertion, the movement needs to be precise and adjustable when the tip is inside the sclera. The depth of the tip should be steplessly controllable for the thickness of the sclera, so the first 0.67mm, to be able to create a wide variety of incisions. After the tri-planar section the depth may be free moving up to a maximum depth of 7mm to prevent damage to other ocular structures. Currently surgeons insert the trocar at 60°, tri-planar incisions would ideally be made using higher angles. For the angled section, the incision angle should be variable between 0-80° in both directions, to improve over the current oblique incisions and allow the surgeon to use the tool on both sides of the head. The center of rotation (COR) should be within the scleral surface to limit translation of the trocar tip. The trocar knife should be a standard 25G trocar that is inserted with the orientation of the blade in plane with the sclera. The functional requirements are visually depicted in Figure 14.

The consistency of the tool is important to make tri-planar incisions in specific. The range of depth in which the steps should be made should accommodate the variation in scleral thickness within the 95% confidence range, this results in consistency requirements for the tool. To have a well sealing planar incision the first vertical sections should be long enough to create a strong flap, but not too long that there is no room for the horizontal section. This point lies around halfway the sclera. The precision should depth with maximal range of 0.05-0.20mm first plane. The middle plane should be between 70-90° to improve over the current angle in oblique incisions. To provide enough surface the length of the middle plane should be in the range of 0.4-0.7mm to provide a surface that is as long as the oblique

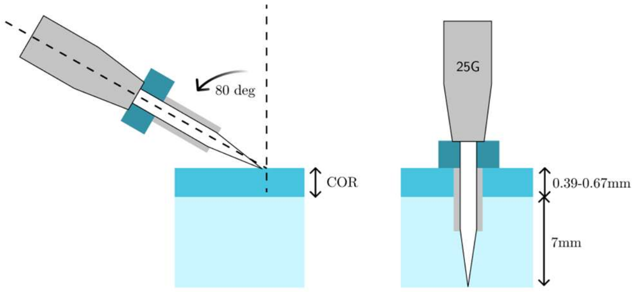

Figure 14: Visualization of functional requirements. See text for more information.

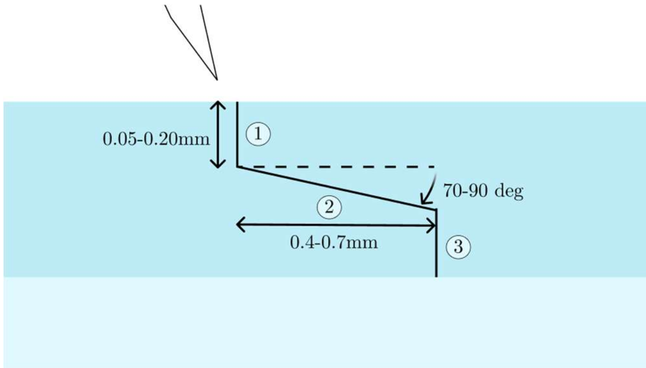

Figure 15: Requirements for the consistency interval of a tri-planar incision. The values should be within these margins 95% of the time. The planes are marked with their respective numbers. See text for more information.

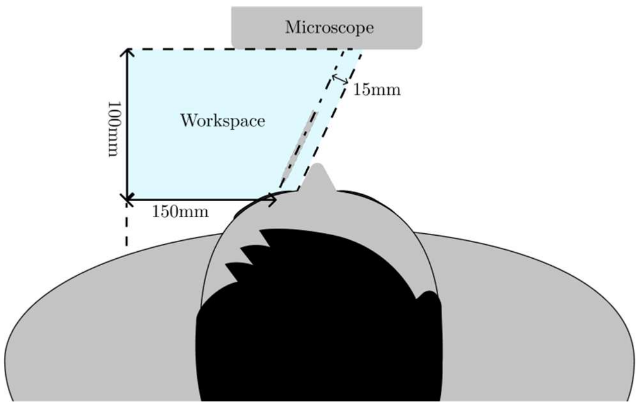

Figure 16: Workspace dimensions during surgery shaded in blue. See text for more information.

incision. The last plane follows from the planes above and does not have additional requirements. The geometry of the incision and the consistency requirements are depicted in Figure 15.

3.2.3 Geometric Requirements

The main factor for the dimensions of a trocar system is determined by the vision system and the face. A trocar system needs to be shorter than the distance between the eye and the microscope. The frontal end must be small enough to clear the nose when positioned on the eye. This allows for a maximal dimension of around 100mm in length and a maximal dimension of the axis of the knife to nose of around 15mm. In the other directions the dimensions are limited to 150mm. These geometric requirements are depicted in Figure 16.

3.2.4 Ergonomic Requirements

The tool should be easy to use for a surgeon, and therefore not put too much strain on the surgeon and allow for precise movement. The surgeons use a pincer grip for precision. Due to high precision required the operating force was based on 1/5th [48] of maximum force presented by NASA [49], resulting in a maximum of 12N operating force. The maximum weight for surgical tools has not been tested specifically, however where hand tools would feel 'just right" at 0.9-1.75kg surgical tools where smaller precision muscles would be used should be a lot lighter. The estimate would be a maximum of 1/5th the weight in surgical tools which is around 180g. This maximum weight will likely easily be met given the geometric requirements. In addition, to make the device easy to use, the mechanism should provide clear visual feedback.

3.2.5 Wishes for a Future Product

If the method is successful, it should be possible to further develop the proposed mechanism to a surgical product. For medical procedures safety is a key factor, therefor the material should be biocompatible. It is impossible to make precise estimates for the cost in this stage of development, however the method should not exclude mass production for disposables and therefore be cheap to produce. Lastly, time in the operation room is expensive and for better adoption of a new method is should not be considerably slower than the current method, which takes less than 30s.

Table 2: Complete overview of the design requirements in three categories and wishes for a future product.

Functional Requirements	
Controlled DOF	Depth and Angle (α)
Maximum insertion depth to prevent damage to other ocular structures	7mm
Adjustable angle range	80° in both directions
Centre of rotation	Within the scleral surface
Placement on pars plana	Visual reference to limbus at 4mm
Type of trocar	25G (0.5mm diameter)
Trocar orientation	In plane with sclera
Force on mechanism	1N
95% confidence interval of depth (In the 1st plane)	0.05-0.20mm
95% confidence interval of angle (In the 2nd plane)	70-90°
95% confidence interval of length (In the 2nd plane)	0.4-0.7mm

Geometric Requirements	
Maximum workspace height	100mm
Maximum workspace width at the nose	15mm
Maximum workspace width elsewhere	150mm

Ergonomic Requirements	
Operatable with a pincer grip	yes
Maximum operating force between index and thumb	12N
Maximum weight	180g
Ease of use	Clear visual feedback

Wishes for a Future Product	
Material	Suitable for future manufacturing in bio-compatible materials
Costs	Suitable for future low-cost mass production for disposable use
Setup time	As fast as possible, but maximally 30 seconds per cannula

3.3 Prior art

3.3.1 Patents

Patent Trocar Insertion Mechanisms

A patent search was performed on a per category basis, to gain some insight in the current developments in trocar design. Four patents [50-53] were found that were relevant and described a trocar insertion mechanism in category (A61B17/3415), ‘Trocars; Puncturing needles for introducing tubes”. All four patents describe a trocar mechanism that can insert trocars on the push of a button. All mechanisms that were found insert in a straight path without steps. The most striking is a patent that describes a mechanism that is able to insert the trocar knife at a higher velocity, triggered by a button on the side [52], visible in Figure 17. This mechanism is strikingly similar to a mechanism Bausch + Lomb presented at the Ophthalmology Innovation Summit of 2016 [54].

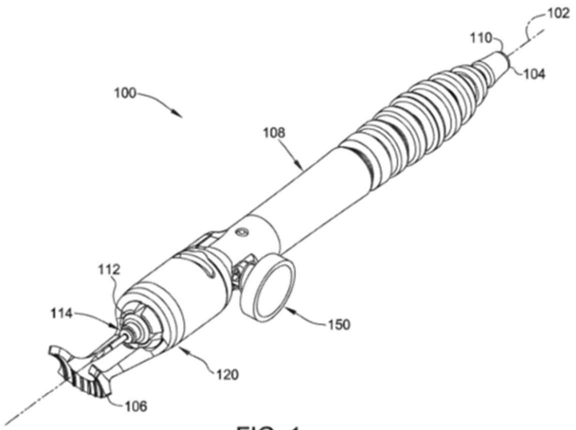

Figure 17: Patent of trocar with a propulsion [52].

The mechanism by Bausch + Lomb proved to be successful at lowering the rise in IOP during insertion of the trocar. However even though the reduction in IOP is drastic, it is regarded as clinically irrelevant by doctors as discussed in Section 2.6.4. Although this was not tested for this specific model, the higher speed might lower the needling forces at insertion. The other three patents in this group described methods to hold cartridges of multiple cannulas to be inserted in sequence.

Patents on Needle Steering

A second search was performed on the category (A61B2017/3405) ‘Needle locating or guiding means using mechanical guide”, searching for a wider range of needling guides in other medical specializations. Within this group there are two types of needle steering, whole needle or just the tip. The first group consist of stiff structures that mostly guide the needle in a straight line.

Most guides are stiff and straight, with no steering [55]. Some do allow movement, but only pre-insertion [56]. One such mechanism is depicted in Figure 18. This is logical, as rotation within deeper tissue would lead to translations sideways along the length of the needle that is further away from the center of rotation. Where in deeper tissue this would have detrimental effects, the exterior position of the scleral path would allow for more rotation of a rigid needle as the distance from the center of rotation can be made relatively small. In addition, after creation of the path using the trocar, a straight and rigid cannula will take its place, applying the same deformation as a straight needle would have during insertion. The current movement the surgeon makes also uses a rigid tool to make the incision. No tools were found that were both steerable during surgery and rigid.

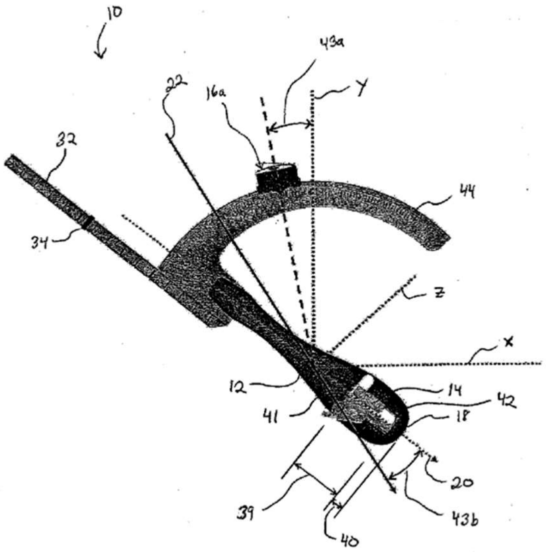

Figure 18: Instrument guide in multiple planes [56].

The second group consist of needles that can be guided in more than just a straight line and these needles are often more flexible. On steerable needles there has been an extensive patent and literature review, which covers 22 patents and makes a distinction between four types of steerable needles [57]. The different groups are, pre-defined and on demand deflection, and the number of rotational planes. Two more recent patents were added to these finding, one patent with flexible needle and steering the shaft [58],depicted in Figure 19, and one with buckling tip [59]. Even though the different steered needles seem diverse due to the number of different actuation mechanisms, the working principle is the same. The needles are driven either by mechanical, thermal, or magnetic actuation. The focus will be on the mechanical steerable needles and these are steered mostly using either a difference in stress or a difference in stiffness. The difference in stress is often with tendon like structures that pull in a asymmetric manner and an example of difference in stiffness would be asymmetric slits in the shaft that deflect when force is applied.

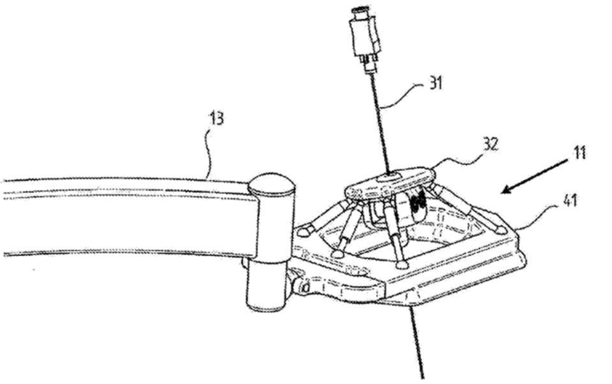

Figure 19; Steerable needle by shaft manipulation [58].

The incision in the sclera requires only a single plane of bending, but both a positive as a negative curvature to create the required wound architecture. And as long as there is some adaptation for different scleral thicknesses, a pre-defined path not a problem. However, the ratio of needle thickness over radius of importance. Pre-curved needles are designed to travel relatively deep into the tissue with a low curvature, for the incision in the sclera a sharp corner with a thick needle is necessary. The needle thickness is in the same order of magnitude as the scleral thickness in which the path is made, it is consequently unlikely that it would be possible to use this working principle in this situation. This leaves only the group of single plane on-demand needles as theoretically viable.

3.3.2 Medical solutions

Z-tracking Technique

For a wider overview in the medical field an interview was conducted with two general practitioners, dr. Suzanne Wolfs. (Personal communication, 4 February 2021) and dr. Eric Roeleveld (10 November 2020). The Z-tracking technique as used in the administration of an oil-based long acting drug [60]. Before the injection, the skin is stretched laterally, and the injection is administered through the stretched skin into the underlying muscle. When it is released, it will return to the undeformed state. The effect is that the straight puncture will deform in a Z-shaped track due to the different displacements on different depths and the sliding of the skin over the muscle as can be seen in Figure 20. This will result in a better sealing puncture and prevent the medication from coming back out. The method allows a doctor to make a complex architecture using a slight deformation and simple straight injection in the skin. Unfortunately, the sclera does not tolerate the required high shear.

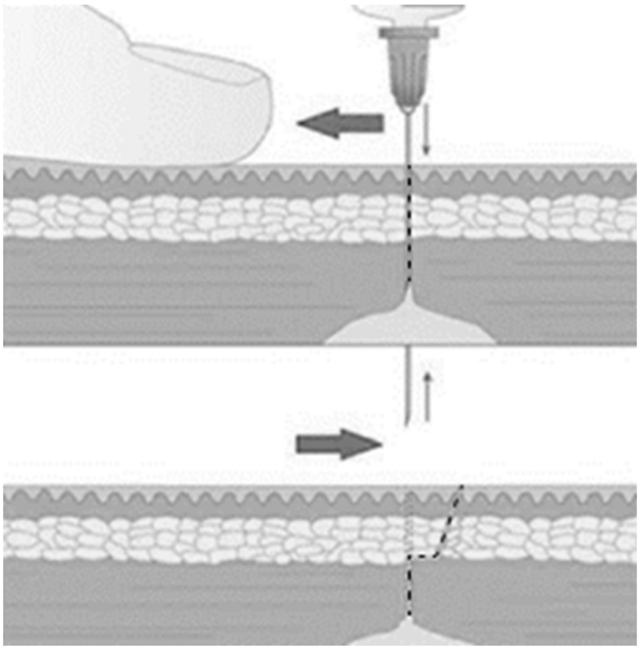

Figure 20: Z-tracking technique used in administration of oil-based drug deposit [60].

Insulin Pump Cannula

An option for diabetes patients is to have an external insulin pump to regulate their blood sugar. The insulin is injected through a cannula that is in place for 2-3 days. To assist patients in placing the cannula there are integrated single use systems available that place the cannula. The system by Medtronic depicted below is pulled and rotated into a loaded position and released by squeezing. The method is so easy to use that patient can place the cannula at home. The device is only capable of inserting straight down, but is interesting as due to its low cost and ease of disposal. A schematic image of this device is depicted in Figure 21.

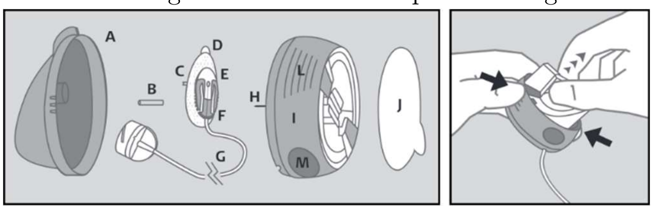

Figure 21: Medtronic Mio Infusion set [61].

3.4 Orientation on Design Directions

The search for a possible solution started with a bird's eye view through orientation in a wide range of methods to create a path though tissue or the sclera in specific, with a tri-planar path in mind. The first step in orientation was a patent search on current trocar insertion mechanisms and patents other needle steering mechanisms. There were only four patents on trocar mechanisms, all of them describing a linear drive mechanism. The patents on needle steering in general provided a range of interesting solutions, however as the trocar remains unaltered no flexible steering mechanism is feasible. Next, an interview with two general practitioners led to another method in which the skin is deformed to create a tri-planar path and prevent leakage and a very easy to use tool to place insulin pump cannulas. The resulting methods can be used for later inspiration in the design. Finally, as guiding and velocity seemed important at first, biological systems were investigated that would be able to combine the two. The chameleon tongue seemed interesting at first, however after it became apparent velocity was of lower importance the method lost its merits, this is described in Appendix C. Based on these findings, a brainstorm session was held to derive new concepts to create a path through the sclera [62]. The results of this session were then structured in Figure 22. Different mechanisms are depicted to the number of degrees of freedom they possess to structure them and generate new ideas on possible different solutions.

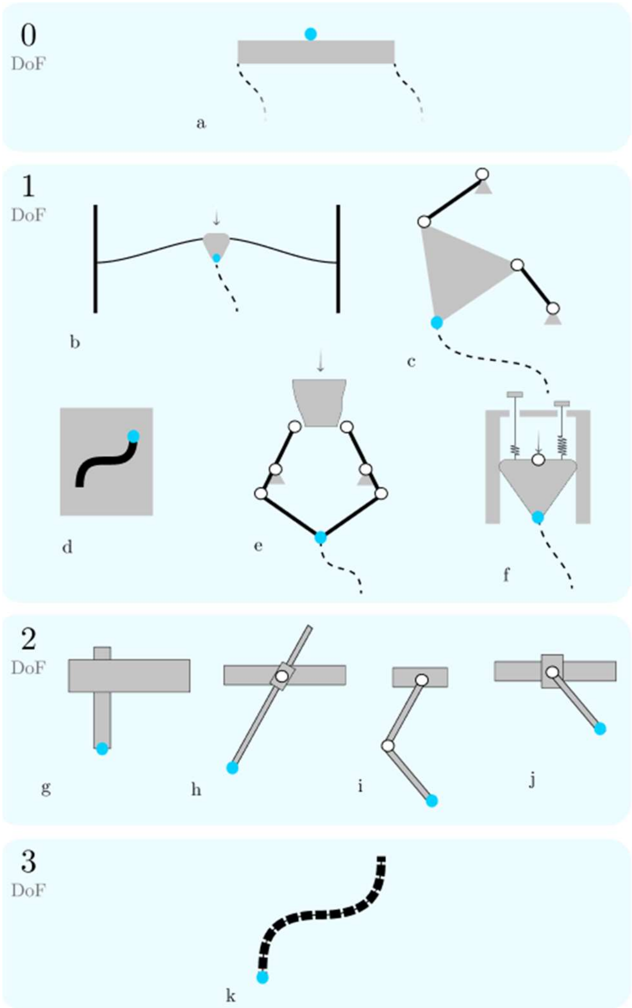

Figure 22: possible solutions against the number of DOF. For more information see text.

a. Moving tissue and keeping the trocar stationary.
b. A buckling beam generates a s-shaped curve when buckling in its second mode.
c. A watt's linkage that is modified will generate a s shaped track.
d. A slot and peon can be designed to create a s shaped track.
e. A cam in combination with a linkage.
f. A body that is rotated based on the minimum in spring energy.
g. Two separate controlled linear axes.
h. One linear and one angular controlled axis.
i. One angular and one linear controlled axis.
j. Two separate controlled angular axes.
k. A set of consecutively links that can be controlled.

3.5 Subsystem Conceptual Design

3.5.1 Division in Subsystems

For the tool that is to be designed, it is important that the geometry is variable over both the insertion depth and the insertion angle to be able to create different variations of the incision geometry. For adjustability it is therefore desirable to separate the angle and depth, leading to two separate degrees of freedom. The possible schematic is depicted in Figure 23. In this system there are four factors of importance. The angle and depth, and the respective reference to the movement. This leads to four sub problems that can be solved independently.

The sub problems

1. Angle guide, position trocar on the desired angle α
2. Depth guide, the depth of the inserted trocar
3. Translation reference, a reference on the ocular surface
4. Rotation reference, the location of the center of rotation within the ocular surface.

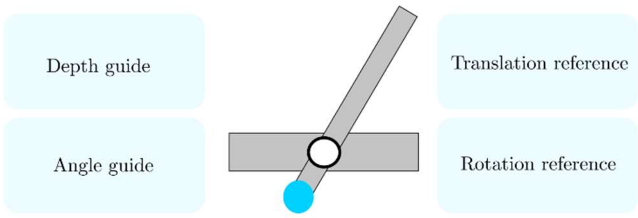

Figure 23: Schematic depiction of the four subsystems.

As the subsystems are relatively independent the solutions can be chosen on a per subsystem basis. The individually chosen subsystems will combine to a final design. Several brainstorm sessions were held, and possible solutions are visualized in a morphological schematic in Figure 24. The design decisions for the subsystems will be discussed in the Sections below.

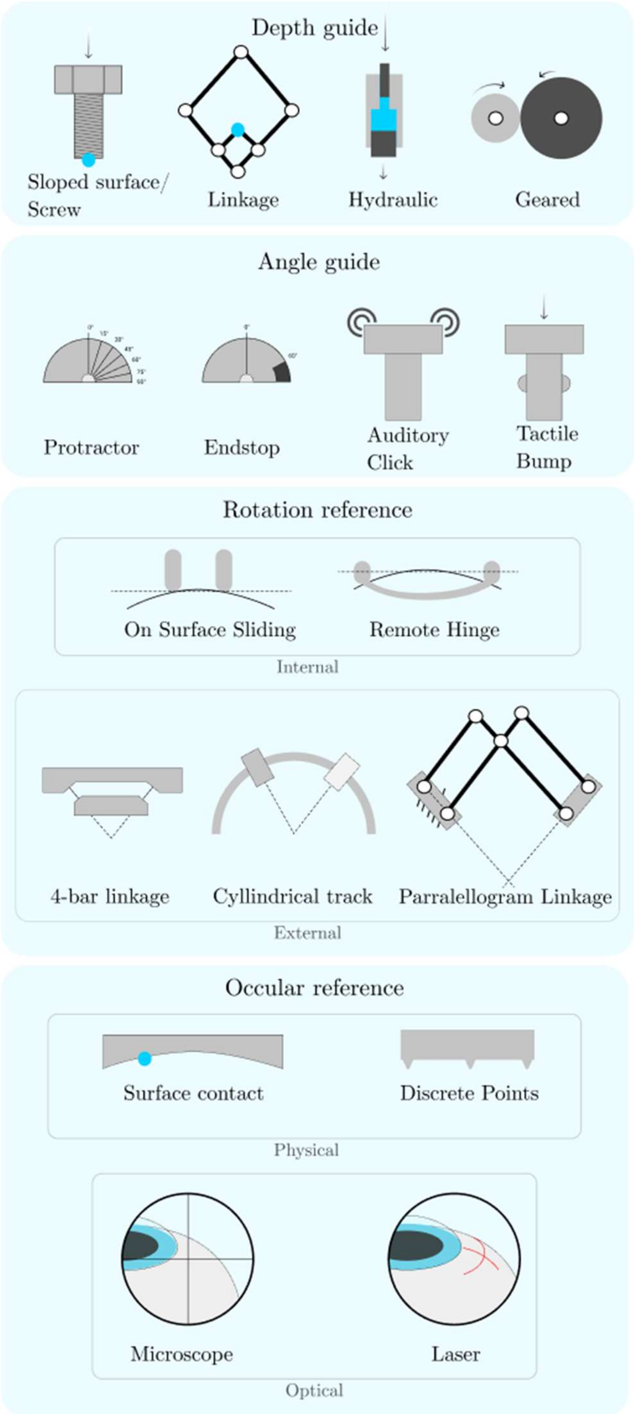

Figure 24: Morphological schematic of the four subsystems. Possible solutions are depicted in boxes of the four subsystems. See text for more information about the solutions and division within the solutions.

3.5.2 Depth Guide

The main function of the depth guide is to enable precise control of the translation of the trocar. In essence this is a transmission problem, where the larger insufficiently precise movement of the surgeons is reduced to a movement that is sufficiently precise. The applicable requirements are the positioning precision in depth and the maximum allowed movement. The mechanisms in the morphological schematic all use some method of mechanical advantage. Two solutions seem promising, a pantograph mechanism and a screw mechanism. A screw mechanism requires an additional system to remove rotation from the tip and the pantograph mechanism is limited by the gear ratio. Both have advantages, the screw can be made self-locking making it safer, however the pantograph system is faster. To make the choice between the two options a more extensive analysis was performed in Appendix B. mainly due to a higher reduction ratio and compacter design the screw mechanism with a compliant guide was chosen for this subsystem, as depicted in Figure 25.

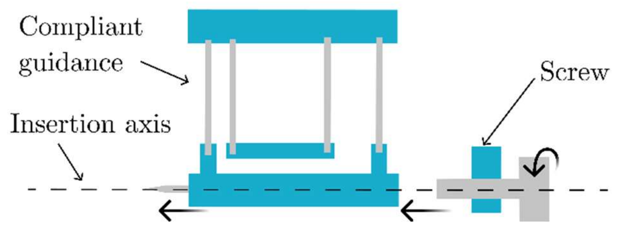

Figure 25: Chosen concept for the depth guide. A compliant guidance actuated using a screw. The dotted line depicts the insertion axis.

3.5.3 Angle Guide

The angle of rotation should be visualized to the surgeon precisely. The most simple and easy to use solution would be an end stop preventing the rotation to go past a predetermined point. However, during the experimental phase of this design the shape of the desired incision might still change. Other forms of feedback are possible such as auditory, tactile, or visual feedback trough a protractor. As the experiments were performed using a microscope, the choice was made to use a digital protractor in the microscope software to determine the angle. Later iterations of the design will most likely use an end stop at the desired angle.

3.5.4 Translation Reference

The translation reference should provide a stable point from which the movement of the trocar can be made. The main difficulty lies in the deformation of the sclera during insertion. The current method of referencing to the eye is visual, using the microscope and using an indenter for reference to the limbus. The surgeon looks at the eye and tries to compensate for the deformation. Unfortunately, this requires a lot of training for the surgeon and is less precise. Maybe in the future this could be aided by visualizing the deformation using laser lines, this would likely be a more complex option. There are more simple mechanical solutions. A full surface contact as in the case of a cup that would support the device on the sclera would reduce the deformation and would likely provide a stable platform. However, a cup covering the whole eye would directly interfere with already inserted cannulas elsewhere in the eye. Therefor a limited support on the region around the insertion was chosen. A semicircle around the insertion location will stretch the sclera into a local flat section. To keep enough support on the eye to stabilize the movement and limit rotation it would be necessary to add more pads, a possible configuration of the pads is depicted in Figure 26. The minimal number would be three pads including partial cup for a stable support that does not interfere with the cannulas. On the partial cup there can be a clear visual marker that the surgeon can use for alignment, as depicted in Figure 26.

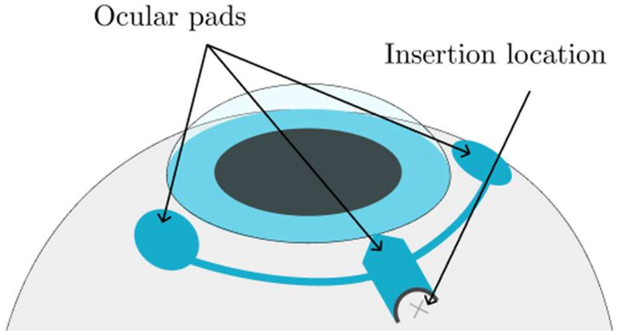

Figure 26: Ocular pads and reference. One pad in the center that flattens the scleral surface and provides a reference to the limbus and two outer pads providing stability during insertion.

The marker should be easy for the surgeon to read independent of parallax. As long as the edge is close to the scleral surface parallax will not be a problem. The design can be chosen dependent on the structural requirements in the detailed design.

3.5.5 Rotation Reference

The center of rotation (COR) should lie inside the surface of the sclera and the axis of rotation is defined by the surface of the eye and the desired insertion location. This placement can be done using two distinct methods. The axis of rotation can either be internal, where the axis passes through the mechanism or external where the axis is outside of the mechanism. In the case of an internal COR the mechanism the curvature of the eye can be used to allow the axis of a joint to be placed inside the sclera. The alternative is an external COR, which would allow for a deeper center of rotation, but would also add a lot of complexity as can be seen in Figure 24 [63]. An internal COR therefor seems favorable. If more room is necessary around the insertion location, the hinge can be moved away. The reduction of stiffness due to the longer arm can easily be compensated for with a stiffer hinge as more space is available. The concept of this subsystem is depicted in Figure 27.

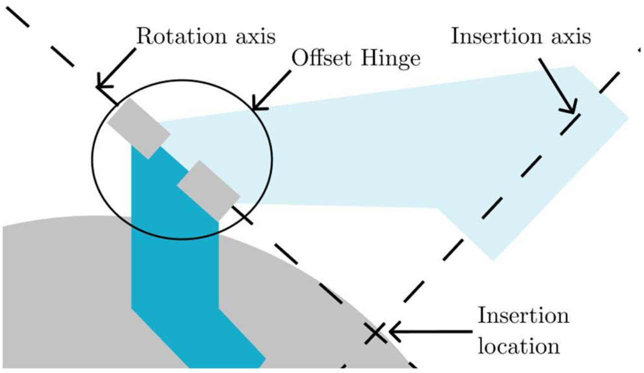

Figure 27: Chosen concept for the center of rotation. A remotely placed hinged with a rotation axis crossing just below the scleral surface at the location where the insertion and the rotation axis cross.

3.6 Final Conceptual Design

A screw mechanism with a compliant guide seems the most promising solution, in combination with a hinge that is placed away from the insertion location placed on the eye using three pads of which one flattens the surface of the eye. The conceptual design is depicted in Figure 28. The dashed lines represent the rotation axis and the insertion axis.

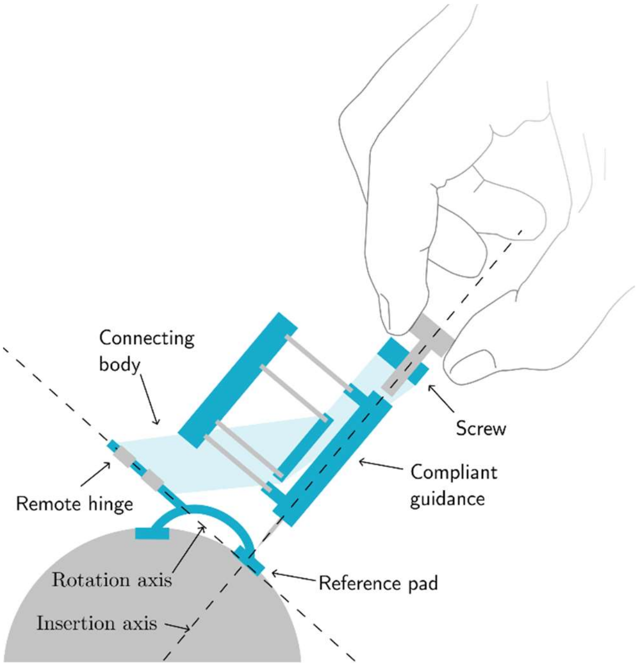

Figure 28: Schematic representation of the final conceptual design. The rotation axis and insertion axis are marked with dotted lines.

4 Prototype

4.1 Prototype Objective

The objective for the development of a functioning prototype is to verify the chosen conceptual design and perform experiments using this prototype. Additionally, manufacturability is evaluated at the small dimensions and tolerances that are required. The result from transformation into a functional proof of concept prototype will be described below. The prototype design consists of an iterative process in which the dimensions are determined, and the design is optimized for manufacturing using 3D printing [64-66]. For the design, the CAD program Solidworks 2019 (*SolidWorks Corp, Dassault Systems, France*) was used. The design per subsystem and the connection between the subsystems is discussed below.

4.2 Prototype Design

4.2.1 Hinge

Ideally the hinge should be as close to the point of insertion to shorten the arm and reduce unwanted movement of the mechanism. However, there is a tradeoff as the hinge itself may not touch the eye to ensure good contact of the support and not occlude the view of the insertion location. The closest the hinge could be placed was 10mm away from the insertion location. For testing is in convenient if the reference can be exchanged, therefor the axis was made using an M3 bolt to enable easy removal. The reference side of the hinge was made 2.9mm to allow the thread to be tapped and the guide side was dimensioned at 3mm to enable a tight but free movement. A render of the hinge is depicted in Figure 29.

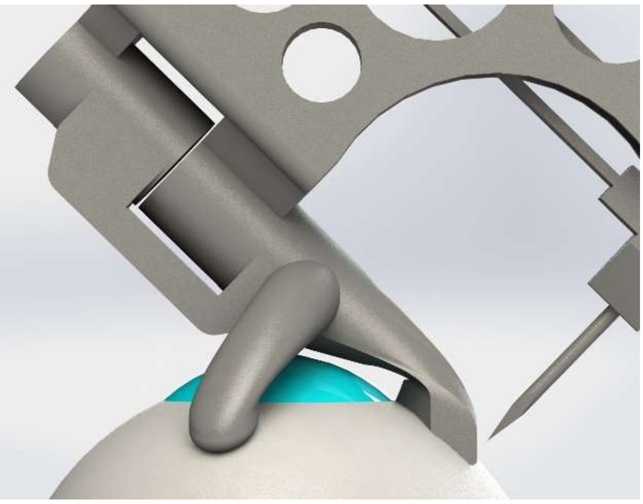

Figure 29: CAD model of hinge viewed from the side. The model is placed on top of a model of an eye.

4.2.2 Flexures and Screw

The dimensions for the flexures were dimensioned using the *Solidworks Simulation* addon in Solidworks and a prototype made on the Formlabs 3B resin printer. The flexures are 15mm long, 5mm wide and a thickness of 0.5mm. The intermediate body and the body in which the trocar was housed were dimensioned where the stress was below 1/10 of the stress in the flexures to ensure deformation is limited. The FEM simulation of the deformation and stress can be seen in Figure 30. 3D printed parts are known for some hysteresis and viscous behavior, to ensure a guaranteed normal force from the spring mechanism to the screw the body in which the trocar is placed is set back 2mm. This will result in 2mm deformation when the trocar touches the sclera. The screw is an M3, which has a pitch of 0.5mm, requiring a full rotation of the screw to puncture the sclera. To allow the mechanism it was necessary to leave large enough gaps for drainage, this was initially 0.5mm but increased to 1mm due issues with parts binding together after printing.

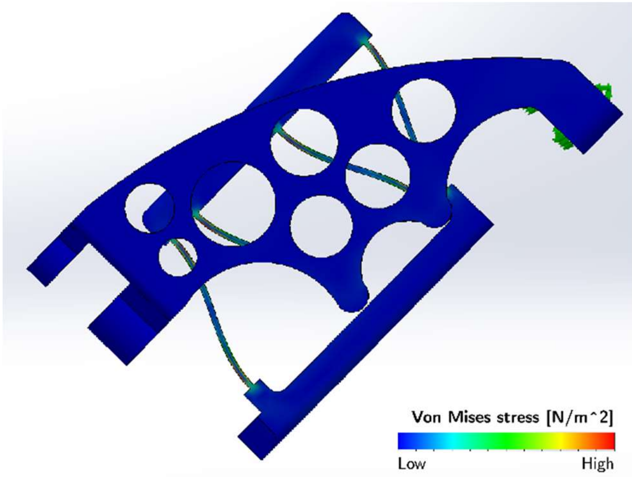

Figure 30: FEM simulation of the deformed state of the mechanism and the stress in the flexures.

4.2.3 Ocular Pads

The pads on the eye provide the necessary stability for the incision. The hole near the tip provides a clear visual reference that can be placed on the limbus and is the required 4mm away from the trocar. This pad is shaped in such a way that the surgeon can easily see the insertion location, even when the trocar is retracted. In addition, this shape will likely help in stretching the insertion location for a more consistent incision. The tips are tapered to prevent interference with the trocar and allow for the full 80° movement from the requirements. The two pads further away from the trocar provide support, especially when the device is tilted. The device was placed on a 3D model of an average human eye, which is similar in dimensions to the porcine eye the device will be tested on [67, 68]. This allowed confirmation that there was enough clearance with the eye, but also visualization of the perspective of the surgeon as depicted in Figure 31. During verification, the device will be tested on flat and cylindrical material as well. For these tests two additional references have been designed, in which the pad around the insertion location is identical. The rest of the reference pad has been redesigned for the differently shaped sample. See verification for more information.

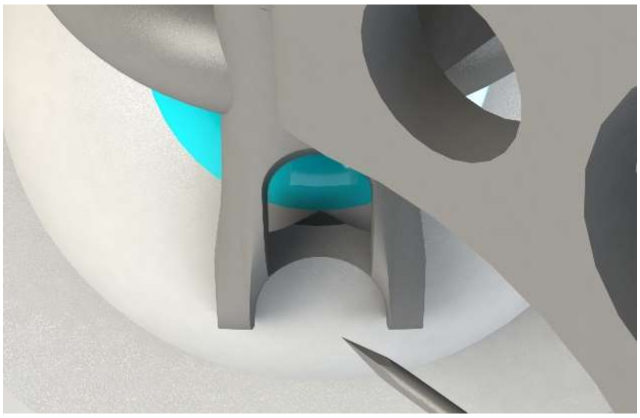

Figure 31: Close up of CAD model of ocular pads from the perspective of the surgeon when aligning the trocar.

4.2.4 Connections

All the subsystems should be connected for the device to function. There should be a connection going from the hinge to the attachment of the leaf flexures and the screw. The connection should be stiff, yet not occlude the vision of the surgeon. The sides have a cutout at the base so the tip can be seen with minimal rotation of the device.

To allow for 3D printing a few modifications were necessary. The clearance is 1mm between the sides and the mechanism, this prevents the guidance from sticking to the sides and aids in drainage of resin during printing. To further aid drainage holes were made in the sides, additionally these function access for support removal after printing. Additional holes were made perpendicular to the hole in which the trocar should be placed, these aid in drainage, but also enable visual feedback when positioning the trocar. A render of the final prototype can be found in Figure 32.

Figure 32: CAD model of final prototype design in isometric view placed on a model of an eye.

4.3 Fabrication and Assembly

Due to the complexity of the concept, the prototype was produced using 3D printing techniques. Even though this production method is currently unsuited for mass production, cost will likely keep decreasing putting it within reach. If not, the device can be redesigned to be assembled from injection molded parts for the body and reference and possible steel sheet for the flexures.

All parts, except for the trocar knife, were 3D printed on Formlabs 3B using 'Tough 1500 Resin". After some experimentation standard printing setting were used except for the supports around the flexures. The print was rotated to avoid intersection of support with the flexures and on the locations where the software did generate support they were moved slightly, resulting a more consistent surface. Additionally, this rotation prevented support between the guiding and the body, making removal easier. The sliced model with the custom supports is depicted in Figure 35.

The trocar knife was made at *DEMO, Delft* using wire EDM. After printing, the trocar knife was positioned in place under the microscope protruding 8mm from the body. It was visually aligned with the body using the drainage holes perpendicular to the insertion as depicted in Figure 33. The part was cured for 60min at 70°C, fixing the trocar into place. After curing two post processing steps were necessary, the rotation axis was drilled out using a 3mm hand drill to enable more smooth rotation and the screw axis was tapped with M3 thread on the other end.

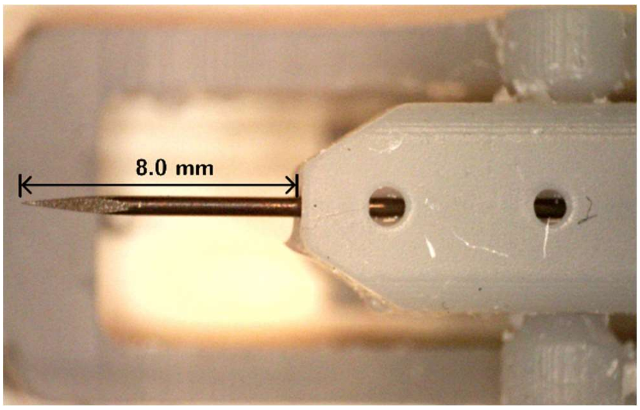

Figure 33: Placement of trocar under microscope

During the design and the prototype phase, the prototype has undergone several iterations, which are visually depicted in Figure 34. The initial prototype tested the feasibility of a compliant guiding mechanism in combination with a screw. Once it was established this would work, the prototype was further enlarged to increase the maximum deflection. The initial cup was changed to three pads, due to interference with pre-

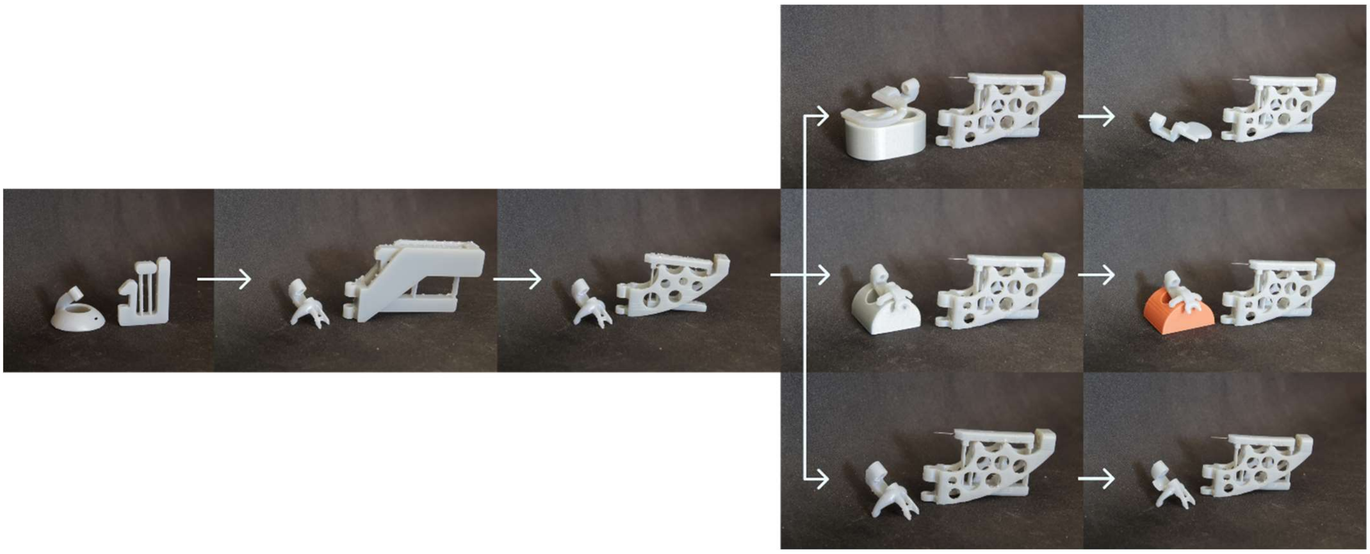

Figure 34: Iterations prototype from earlier prototypes (left) to the final versions (right)

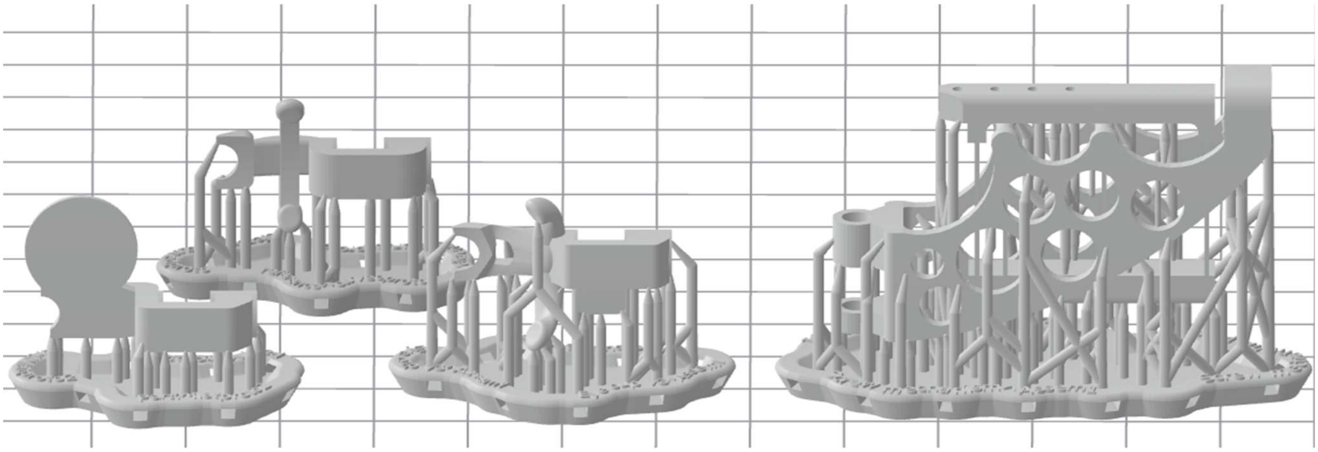

Figure 35: Sliced model of three different references (left) and the guidance (right)

inserted cannulas. This prototype was not able to move after printing due to compliant mechanism sticking to the side. The next step was to add holes to improve printability due to better drainage of the resin and improved axis to remove support material from in between the flexures. In addition, material was trimmed around the insertion to create a clear the line of sight. Finally, the different reference parts for the different test were developed and improved, providing better support during the verification.

5 Verification

5.1 Verification Objective

The main objective of the verification is to verify the ability of the newly designed tool to create tri-planar incisions consistently and conform the predetermined requirements. Secondly, the leakage of the incisions should be tested to determine the sealing capabilities of the tri-planar incisions.

5.2 Experiment Design

5.2.1 Introduction

There are several factors that can influence the consistency of the incision. The interaction between the tool and the tissue is likely the most critical factor. Different levels of interaction can be experimented with consecutively. Initially, the mechanism should be tested in limited material deformation to test the consistency and structural properties of the device. This can be done by inserting the trocar in a slab of silicone that is fully supported from the bottom. The path the trocar travels can be analyzed from the side, providing an indication for the consistency of the path. For the second test the deformation present during insertion can be simulated on a phantom eye, an artificial eye that is geometrically similar to a biological eye. Like the human eye, it will deform when the insertion force is applied. This test will evaluate if the incision shape can still be made in this deformed configuration. In addition, the phantom eye allows to determine the leaking and therefor sealing of the tri-planar incision. Lastly the same test as on a phantom eye can be repeated on a porcine eye, to test the leakage on biological material of which the properties are more like the human eye. For the tests, the tri-planer incision was based on *Spandau et al* [9] as depicted in Figure 9. The angle depicted in Figure 9 was lowered from 80 to 70° due to interference with the table in the test in flat material. This allowed all specimens to be tested with the same architecture and enable comparison between the tests. The incision was made using the following steps:

1. Lowering of the trocar to the point where is just touches the surface.
2. 0.5 rotation on the insertion screw (0.25mm).
3. 70° device rotation.
4. 1.25 rotation on the insertion screw (0.625mm).
5. Returned to 0° device rotation.
6. Insertion up to 7mm.

To compare the leakage of tri-planar incisions, additional straight and oblique incisions were made. These incisions were made by placing the device on the material, straight or under 60° respectively and inserting the trocar all the way. The hypothesis is that the device will perform very consistently on the flat silicone material, and almost as consistently on the deforming material of the eye phantom, due to the design of the reference creating a locally flat section. In the leakage test the straight incision will leak most, the oblique incision will perform a lot better under pressure, closely followed by the tri-planar incision.

5.2.2 Flat Test

Method

The goal of this test is to analyze the consistency of the method. The tool was positioned on top of the material around 1-2mm from the edge and the tri-planar incision was made. This was originally done 6x with ink on the tip to stain the incision but continued without ink to improve view of the entry point. The experiment was repeated 11x for the 2.0mm thick material to see the path of the trocar inside the eye and 12x for the 0.5mm thick material where the initial touching of the surface was aided by a microscope. After all incisions were made on the strip microscope pictures were taken of the incisions. From these images the depth of the first plane, the angle of the second plane and the length of the second plane were measured. From these values the consistency interval was de termined.

Facility

Transparent silicone rubber with a hardness of 60 shore A from *Rubbermagazijn, Zoetemeer* has been used as the scleral substitute. This material has mechanical properties most closely resembling that of the sclera [69]. The silicone sheet is produced in 0.5mm and 2mm thickness and both have been tested. The material was cut in to 10x50mm strips. During the test it was suspended by three layers of the 2mm rubber to accommodate the length of the trocar after puncture. Images were made using digital microscope (Dinolite edge 3.0) positioned horizontally from the material and analyzed using DinoCapture. An image of the setup is included in Figure 36.

5.2.3 Phantom Test

Method

The goal of the phantom test is to determine transfer of the performance to a situation with more deformation and to compare leakage between different incision architectures. The path was examined under the microscope similarly to the flat test. The leakage was tested using a modified Seidel test, in which the incisions are pressurized by applying pressure with forceps and the surface is inspected for leakage of a fluorescent tracer fluid. [70] This test is common after surgery to determine leakage and therefor the associated need for suturing. As opposed to the standard test, no fluorescent was used, and the pressure was applied on the cannula instead of applying pressure to the eye with forceps, to enable more consistent comparison between incision on the same phantom.

The trocar-cannula prototype was placed on the phantom with the pads and aligned with the cavity and gently pressed on the surface, ensuring good contact between all pads. The trocar was aligned with either the center or 3-5mm left or right of the center, creating a total of three locations per phantom. The trocar is lowered by turning the knob to the point where it first touches the silicone layer. Then one of three incisions was made, tri-planar, oblique, or straight. Using a plunger on the syringe the pressure in the phantom was increased till leakage was visible through the incisions, the amount of leakage was captured using the microscope. As the silicone material is hydrophobic the fluid from the leakage forms spherical droplet at the incision. Using the droplet diameter on the microscope image, the leakage was calculated using the volume of a sphere formulated in Equation (4), in which D is the droplet diameter.

$$V = \frac{4}{3}\pi\left(\frac{D}{2}\right)^3 \tag{4}$$

Figure 36: Experimental facility flat test.

Figure 37: Experimental facility phantom test.

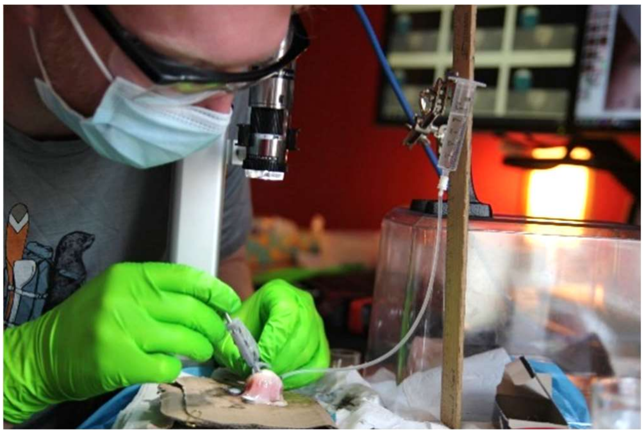

Figure 38: Experimental facility wet lab.

Lastly the silicone surface was cut from the cylinder using a scalpel and a section of 3x10mm around the incision is cut and placed under the microscope. This was repeated 3 on three eye phantoms to create 9 incisions. The order and positions were different on all phantoms to remove systematic error.

Facility

Eye phantoms were made by 3d printing cylindrical cups on a 'Prusa i3" out of PLA and gluing silicone rubber on top creating a watertight cover. Care was taken not to contaminate the rest of the silicone surface with glue. There is a hole in the bottom of the cups through which they are filled using a syringe. When the phantom is fully filled and without air bubbles the hole was sealed using double sided tape. The instrument was unchanged with respect to the previous test, except the flat pad was switched for a cylindrical pad.

The pressure was kept constant by inserting a 23G trocar at the edge of the cut-out and connecting it to a reservoir with a silicone tube. The reservoir was elevated to 202mm water level above the incision, which produces the equivalent pressure of 15mmHg normally present in the eye. An image of the setup is included in Figure 37.

5.2.4 Wet Lab Test

Method

The wet lab test aims to find out how the properties of the phantom test translate to biological material. The test is similar to the phantom test with three differences.

1. To visualize leakage, it was necessary to stain the vitreous humor. This was done using India ink particles which are representative for ingress of bacterial matter [70].
2. No pressure was added to increase the leakage it was already visible and as a precaution to ejecting biological material from the eyes.
3. The water in the syringe was switched for physiological saline solution to prevent changes in the material due to a difference in osmotic pressure.

The eyes were pinned through the muscles to a piece of cardboard to keep them stable on insertion. A 23G trocar was used to place a cannula on one side of the eye for pressurization. Ink was injected through the cannula and the pressurization tube was attached. The tool was placed on the surface of the eye and gently pressed for solid contact and inserted. Three different incisions were made, straight, oblique and tri-planar. After the incisions, the surface was massaged to close the wounds and after 2 minutes the eyes were inspected for further leakage and recorded using the microscope. These steps were repeated for a total of 3 eyes.

Facility

Ex-vivo porcine eyes were ordered at butcher *Slagerij Leo van Vliet, Delft.* The eyes arrived frozen and were slowly defrosted at room temperature the night prior to the experiment. The instrument and the pressurization were unchanged with respect to the previous test, except the cylindrical pads which were switched for spherical ones. An image of the setup is included in Figure 38.

5.3 Results

5.3.1 Flat Test

Within the first six incisions that were made using ink on the tip, none showed the desired thri-planar structure. The ink was successful at staining the incision to around the half the thickness of the material as can be seen in Figure 41. In this incision two problems presented itself, the tool would not retract after it had been left in the extended position for a few minutes and the ink occluded the entry point and made it difficult to gauge whether the tip had touched the surface.

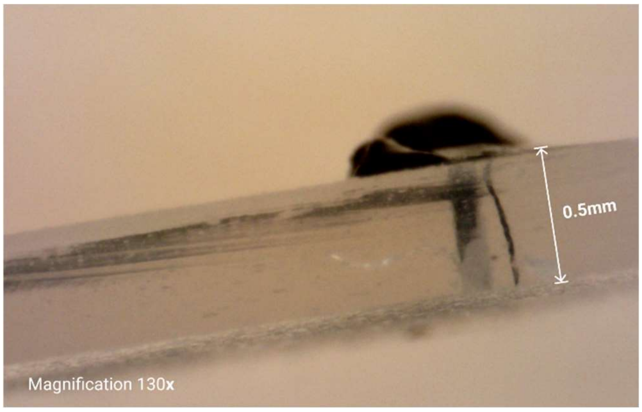

Figure 41: Microscopic image of initial test with prototype. Test 1.1, other images found in Appendix E.

The second set of 12 incisions was done in 2.0 mm thick material, an example of the microscope images is depicted in Figure 39. All incisions (100%) showed a tri-planar incision within the first 0.5mm. The deviation of the first plane length was relatively large, with a value of 0.05mm. In Figure 39, the second plane starts flat curves down slightly. The last plane starts with a slight angle but straightens over the depth.

The last set of 11 incisions was done in 0.5mm thick material, an example of the microscope images is depicted in Figure 40. All incisions (100%) showed a tri-planar incision within the first 0.5mm. As opposed to the incision in 2.0mm material the first plane had a much more consistent depth, with a standard deviation of 0.02mm. The deviations and means of the

Table 3: Deviation and mean of incisions in flat material.

2.0mm (n=12)	STD [mm]	Mean [mm]
Depth (1st)	0.02	0.19
Angle (2nd)	3.53	80.09
Length (2nd)	0.09	0.73
0.5mm (n=11)	**STD [mm]**	**Mean [mm]**
Depth (1st)	0.02	0.13
Angle (2nd)	3.13	75.36
Length (2nd)	0.12	0.45

Table 4: 95% confidence interval in 2.0mm and 0.5mm

2.0mm (n=12)	Min	Max
Depth (1st)	0.02 mm	0.35 mm
Angle (2nd)	76.9°	83.3°
Length (2nd)	0.65 mm	0.82 mm
0.5mm (n=11)	**Min**	**Max**
Depth (1st)	0.06 mm	0.19 mm
Angle (2nd)	72.5°	78.3°
Length (2nd)	0.35 mm	0.54 mm

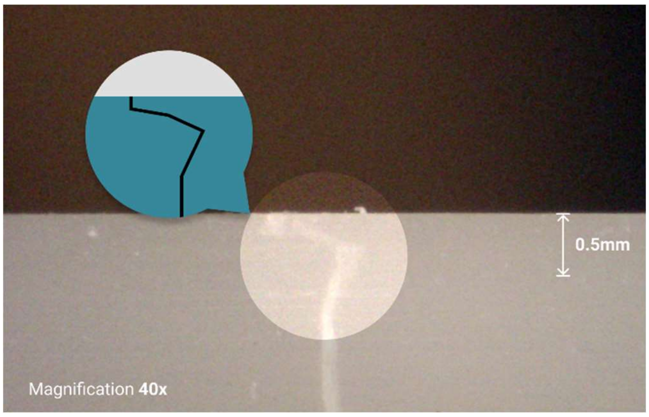

Figure 39: Microscope image incision in 2.0mm silicone. Left of the incision is a schematic trace of the incision path. Test 2.1, other images found in Appendix E.

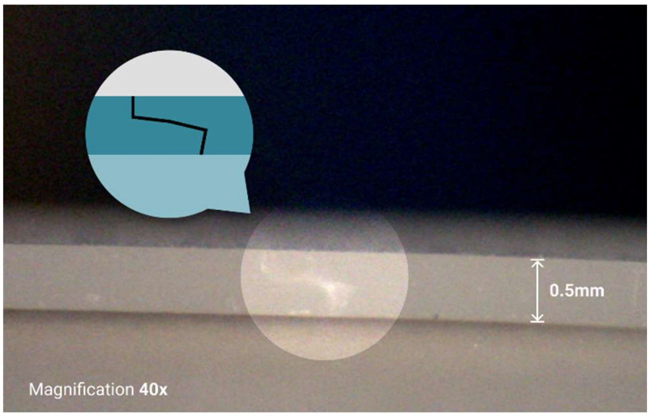

Figure 40: Microscope image incision in 0.5mm silicone. Left of the incision is a schematic trace of the incision path. Test 3.11, other images found in Appendix E.

Table 5: Leakage in eye phantoms after different incisions

Leakage [µl]	straight	oblique	tri-planar
Phantom 1	5,96	34,53	3,48
Phantom 2	18,99	0,49	0,14
Phantom 3	17,48	2,31	10,42

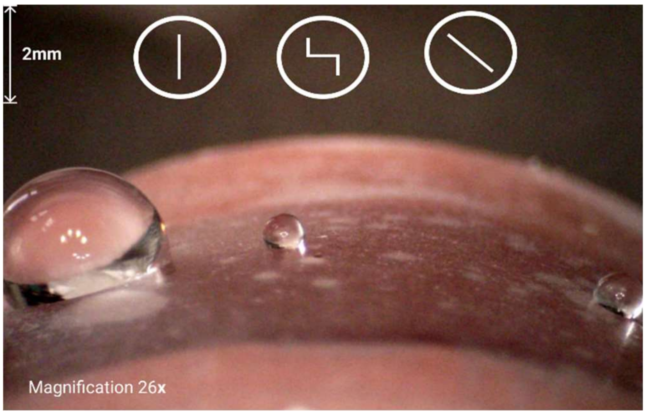

Figure 42: Leakage test of eye phantom, with the type of incision depicted at the top of the image. Test 5.2, other images found in Appendix E.

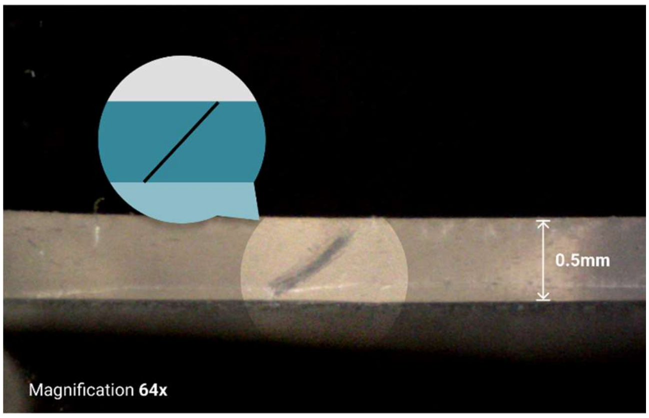

Figure 43: Oblique incision in phantom. Left of the incision is a schematic trace of the incision path. Test 4.2, other images found in Appendix E.

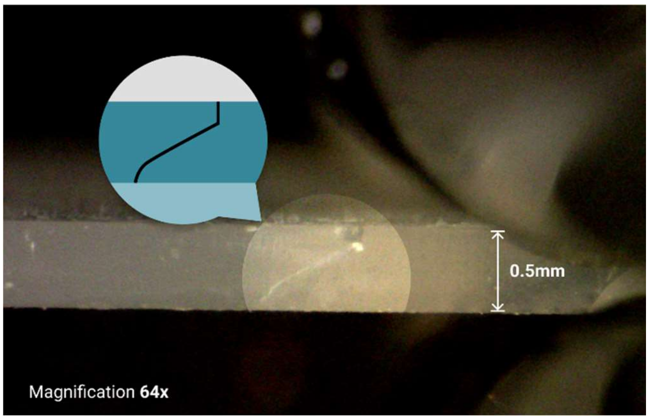

Figure 44: Tri-planar incision phantom. Left of the incision is a schematic trace of the incision path. Test 4.9, other images found in Appendix E.

measurements can be found in Table 3. All images of the incisions, as well as the measurements can be found in Appendix E.

The confidence interval from a sampled set of measurements. The sample size is small, therefor sample mean might differ from the population mean. To compensate instead of a normal distribution a t-distribution is assumed, which has ''fatter tails'' due to the larger uncertainty of the mean. The t-value for (n=11) and (n=10) at a 95% confidence interval are 2.23 and 2.26 respectively [71]. The resulting 95% confidence intervals are listed in Table 4.

5.3.2 Phantom Test

The eye phantom was first tested for leakage, an example result can be seen in Figure 42. The first phantom encountered some interference with insertion during on the oblique incision. There was a high leakage on this oblique incision, however there is no clear abnormality in the incision as can be seen in Figure 43. In this phantom the other two incisions are almost equal in leakage as can be seen from the fluid egress in Table 5. Second phantom showed significant leakage on the straight incision, and the other incisions held well. The third phantom both straight and tri-planar incisions showed significant leakage, even though the tri-planar incision was visually successful as can be seen in Figure 44. The oblique incision sealed well even though it was more oblique than was aimed for.

The tool was able to create the desired incision architecture successfully in all three phantoms, however this did not always lead to a lower leakage, as can be seen in Table 5. Apart from the first test the oblique and tri-planar incision both clearly outperform the straight incision, however between the two there is no clear difference, and the results are not fully consistent. All incisions and leakage in the phantom tests can be found in Appendix E.

5.3.3 Wet Lab Test

Insertion of the cannula using the 23G trocar was a lot tougher than expected, especially as the IOP in the eyes was very low before pressure was applied though the cannula. There is a clear difference in toughness with the phantom. Insertion of the trocar in the tool also lead to severe deformation of the eye, larger than in the phantoms. The first eye did show some leakage on the straight incision, but only a very little but on the tri-planar and oblique. In the second and third eye the straight incision was also leaking the most, and there was some leakage coming from the other two as can be seen in Figure 45.
The difference between straight and oblique is larger in the ex-vivo porcine eyes than in the phantom test, as can be seen in the Table 6 and Figure 45. Again,

Table 6: Ranked performance of incisions in ex-vivo porcine eyes going from lowest leakage to highest, based on visual ink egress from the incision under the microscope.

	1.	2.	3.
Phantom 1	Oblique	Tri-planar	Straight
Phantom 2	Tri-planar	Oblique	Straight
Phantom 3	Oblique	Tri-planar	Straight

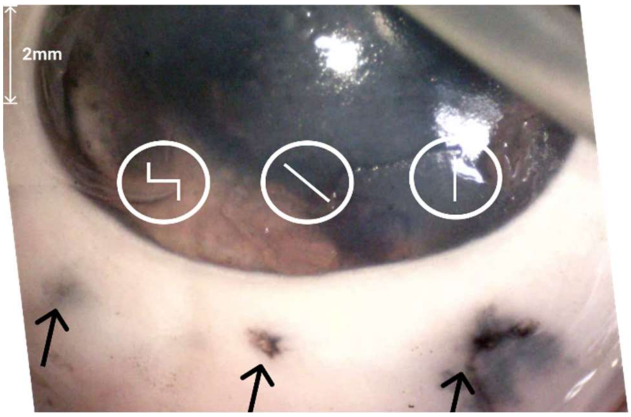

Figure 45: Ex-vivo porcine eye after three incisions using the prototype, with the type of incision depicted in the circles. Incisions marked with black arrows. The darker spots mark ink egress from the incision. Test 6.3, other images found in Appendix E.

the performance of oblique and tri-planar is close together and there is no convincing best architecture. An overview of all test results in the ex-vivo porcine eyes can be found in Appendix E.

5.4 Discussion

5.4.1 Flat Test

In this Section the result presented in the previous Section will be discussed. The implications of the experiments on the study as a whole will be discussed in the next chapter. The initial tests on the flat silicone sheet highlighted the problem that it was difficult to see the exact point where the trocar entered the sclera. In the first test the material was already fully penetrated by the "touching", this was worsened by the trocar already being slightly protracted applying extra pressure on the silicone. This was solved by using a microscope to position the trocar on the silicone, just like in the current eye surgery where a microscope is used during positioning. In the third test the tool was able to effectively create a tri-planar incision architecture. The confidence interval of the test in 2.0mm was larger than the confidence interval in 0.5mm. This was likely due to more experience with aligning the trocar on the silicone surface. The spread in 2.0mm silicone was larger than the requirements allowed. The confidence interval of the test in 0.5mm silicone does conform to the requirements. Interestingly, the start angle of the incision is flatter than the insertion angle. This difference is likely caused by the moment of the trocar just after entering, causing a rotation of the surface. Another deviation is noticeable after rotation in to the third plane. The path angle rotates more than the trocar rotation and straightens down over the depth. This deviation could be through a deformation due to the shear force of the needle. This causes a deformation difference through the depth of the silicone. When the trocar punctures straight through the deformed material, the path will deviate.

5.4.2 Phantom Test

The phantom test showed that the tool is still able to consistently create a tri-planar incision, despite the larger deformations of the material during insertion into a phantom eye. However, the tri-planar incision architecture did not always lead to a lower leakage. The hypothesis was that the straight incision would always perform worse than an oblique incision, which was not the case for the first phantom test. This might have been due to the extra movement during insertion due to interference with the cannula. Based on the leakage test, it is likely that the tri-planar incision performs better than straight incision, however the test is indecisive whether it outperforms the oblique incision. A larger number of samples would be necessary to differentiate based on statistics.

5.4.3 Wet Lab Test

The transfer from the artificial silicone material to biological material went acceptable. The trocar had a greater difficulty puncturing the sclera as opposed to the silicone material. It was tough for the operator apply this force. The trocar forces felt higher on the 25G trocar than the 23G trocar used for insertion of the cannula for pressurization. This would suggest that the trocar produced by DEMO was not as sharp as the trocar made by DORC or had become blunt after the punctures in silicone. The higher forces on the trocar caused higher deformations during puncture and likely a less precise incision. The eyes were very carefully defrosted; however, the material properties might have changed over time, nonetheless. In addition, the origin and age of the eyes is unknown adding additional variables that could affect the properties. Leakage in the first eye was low on all incisions. This could be due to the properties of the sclera, or potentially due clumping of the vitreous humor clogging the pressurization. In the other two eye tri-planar seems to perform better than straight, but there is not enough evidence for to conclude if oblique or tri-planar incisions perform better.

6 Discussion

6.1 Experimental Recommendations

During this study, a method for the creation of tri-planar incisions was explored to find its potential in reducing post-operative leakage in vitrectomy. To evaluate the potential of this method a functional prototype of a device was developed to consistently execute the procedure. The experiments were successful in testing the incisions, however there is several improvements that can be made in future work.

Firstly, it is recommended that the test is improved on by adding OCT, the imaging method that is used after surgery to visualize the incision architecture, and inspect the ex-vivo porcine eyes. This would allow for comparison of the architecture and the resulting leakage and evaluation of the of the interaction between architecture and fluids. Instead of ex-vivo porcine eyes, it would be possible to keep experimenting using an artificial material. However, a different material, more like the biological variant would have to be found to better represent the tough fibrous structure of the eye.

Secondly, only a single type of tri-planar incision was tested. The incision architecture was chosen based on the limited information available and could very well not be optimal yet. The developed tool provides all the means to create different architectures, and this could very well be used in a future experiment. Using a higher angle on insertion it might be possible to create better sealing incisions or it might be possible to design and test a whole new shape.

Thirdly, the leakage test should be improved to distinguish between oblique and more elaborate incision architectures. The differences in leakages are small and the performed Seidel test could not provide conclusive evidence. There are likely other factors of influence on leakage other than incision architecture alone, for instance the surface roughness inside the incision. A rougher surface could lead to voids through which fluid could flow or the surface could increase friction inside the incision keeping the incision from deforming, these effects should be measured. Furthermore, visual leakage alone might not be the only method of ingress of bacterial mater into the posterior chamber. The "suction pump mechanism" might cause the incision to pump fluid from the outside to the inside of the eye without leakage [41]. A small cavity within the incision might start pumping fluid due to repeated deformation, like a bellow pump. In these cases a seidel test, which only test for visual leaking, might not be sufficient to distinguish different architectures [70]. In case of the wet lab test this could possibly be solved by a more precise measurement of the number of milliliters of fluid egress.

Fourthly, this experiment reemphasizes the importance of blade sharpness. The force on the trocar during insertion in the ex-vivo porcine eyes felt very high and caused significant deformation. The trocars made at DEMO were barely sharp enough to puncture the sclera. It recommended to use a sharper blade on the trocar tip to reduce the forces and resulting deformation.

On the long term, if the further experiments prove to be successful it could be interesting to experiment with different architectures in-vivo and the effect on complications. However due to the high requirements for experimentation in patients this would be a lot further in the future.

6.2 Design Recommendations

The prototype held well during the experiments and lasted for the entire 47 punctures during the experiments. The design meets the functional, geometric, and ergonomic requirements. The wish for setup time was not met as the insertion of each cannula took more than 30 seconds each.

There are still several changes that could be made in the design to further improve the performance. Firstly, the issue with hysteresis in the flexures should be tackled. The current design accounted for 2mm of permanent deformation of the flexures. When the device was left in the protracted position for a few minutes, this limit was exceeded. It is recommended to either increase the travel to account for the larger permanent deformation or select a material that has a lower creep. The material for the flexures could be replaced by a metal to achieve this.

Secondly, the forces and deformation on the mechanism were larger than expected, to the point where the reference sometimes lost contact with the sclera. The easiest solution would be to improve the geometry of the blade to lower the forces. For this a better understanding of the force interaction of the trocar blade and material is necessary. In addition, the reference could be redesigned keep contact with the sclera in the presence of higher deformations.

Thirdly, inherent to the shape of the current trocar the blade is optimized for straight path incisions. Currently when rotating the cutting-edge travels in a 3d shape, which might not lead to an optimal sealing wound. Blade geometry could possibly be improved for rotations, by shortening the length of the bevel. The counterargument to this would be the reduction in sharpness due to a blunter bevel.

Fourthly, the incision of the trocar after the tri-planar incision was slow and there is room for improvement. A future version could feature a mechanism that enables unrestricted and faster insertion once the precision in less necessary after the three planes. This could for instance be a mechanism that decouple from the screw mechanism and extend, rapidly inserting the remaining few millimeters, for instance using a multi-stable mechanism as described by *Zanaty et al* [72]. The area where the speed can be increased is depicted in Figure 46.

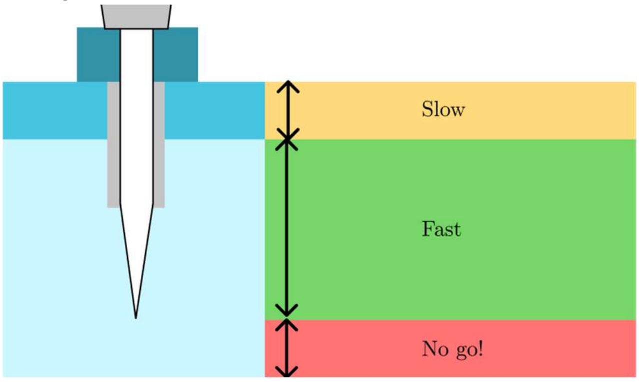

Figure 46: Improved velocity profile for trocar knife to lower insertion time. After passing the sclera (yellow), the trocar can speed up (green) and stop before hitting other ocular structures (red).

Lastly, although not impossible the device was difficult to operate using a single hand. The ergonomics of the device should be improved to make the device easier to use. In addition, this improvement increases the consistency of the incision due to more controlled movements of the device. A possible solution would be to change the grip of the surgeon and add holes through which the ring and middle finger could be placed for added control. In addition, this would place the center of gravity of the device within the boundaries of the hand lowering the operating force and increasing precision. A possible embodiment is depicted in Figure 47.

Figure 47: Design suggestion for a future prototype to improve stability during insertion by adding a hole for the ring and middle finger.

6.3 Study Limitations

The main limitation of this study is the large uncertainty on the mechanics of the sclera during puncture and after extraction of the trocar, and the effect of incision architecture on leakage. Computer modeling of trocar insertion has been attempted, but remains difficult due to the non-linear nature of the sclera [23]. The prototype in this study could provide a first step in evaluation of the properties of paths, the resulting incisions, and the effect of leakage of these different incisions. More in-depth research on these topics in scleral mechanics are needed.

The study has had an explorative character, covering an in-depth investigation with surgeons, instrument design, prototype fabrication and evaluation, with the main goal of investigating if a new method of creation of incisions has potential for further research and development. This has resulted in a very broad range of insights, but limited in-depth assessment of some directions.

6.4 Future Vision

The designed surgical device that can make a tri-planar incision using a new method. If this incision proves to be successful, the device should be further developed. As discussed in the interview with surgeons and stakeholder analysis (appendix B), the surgeon values a quick and easy way to place the cannula, that reduces the risk of complications. The vision of a future method includes a consistent and simple method. Consistency would increase over time as more knowledge is gathered using the device to improve incision architecture and improve our understanding of the mechanics of insertion. This could lead to a uniform 'best' architecture in eye surgery, as opposed to the wide variety in incisions currently used. The simplicity of the tool could possibly evolve into a one-click method in which an architecture is selected, and the cannula is inserted with a single press of a button. The surgeon will spend less time placing cannula's whilst having a lower risk of complication for his or her patients.

7 Conclusion

The goal of this work is to: **"Design and verify a new, reliable and easy to use method to create tri-planar incisions for scleral cannulas to limit leakage after extraction of the cannula."** This question was answered through a set of five research questions. The findings on each question are summarized below.

First, the circumstances during the surgery were analyzed, which provided critical insights for the development of the tool from a technical standpoint. Next, interviews with different surgeons focused on the user perspective to explore the critical factors of influence on a well sealing incision. Taking both perspectives into account, the most important factor that can be improved upon is the incision architecture.

Secondly, these findings were translated to a set of requirements for a surgical tool to be developed. As a result, these can be used to evaluate and verify designs on the factors brought to light in the first research question.

Thirdly, during a creative phase, several design directions were explored. A device with two degrees of freedom, one for the angle and one for the depth of insertion, was preferred due to its simplicity. To guide the further design, the solutions were divided in four subsystems, namely the magnitude and reference of the depth and the magnitude and reference of the angle. Solutions were derived on a subsystem basis and evaluated using the requirements. A combination of the subsystem solutions led to a final conceptual design. This design was consequently dimensioned leading to an initial prototype design, which was iteratively improved.

Fourthly, the prototype design was verified using both artificial as well as biological material, to test the created incision architecture and the effectiveness of the new incision. The tool was successful in making the tri-planar incisions in artificial material, as all three planes were clearly visible when observed through the microscope. In the leakage test, the oblique and tri-planar incisions both performed better than a straight incision. More experimentation with larger sample sizes, better imaging, and more representative material is necessary to distinguish between the oblique and tri-planar incision.

In conclusion, the research goal has been fulfilled and a functioning new method has been designed and developed. The newly designed tool enables a new incision architecture for surgeons and paves the way for further research.

8 Acknowledgements

First of all, I would like to thank Kirsten Lussenburg for her enthusiasm and support as a daily supervisor. Secondly, I would like to thank Paul Breedveld for all his support and guidance in this process. For the medical advice and suggestions, I would like to thank Peter van Etten, Niels Crama, Sander Keijser, Eric Roeleveld, Suzanne Wolfs and Chantal Staring. I also want to thank Mart Gahler for the positive contact with DORC and the insights he provided in the design of trocar systems. For the help during the experiments and visualizations in the report, I would like to thank Felix Akkermans. Lastly, I would like to thank my friends and family for all the support throughout the process and keeping me sane.

Bibliography

1. Lussenburg, K. 2020.
2. Marieb, E.N. and K. Hoehn, *Human anatomy & physiology 10th edition.* 2016: Pearson education.
3. Scott, A.W., et al., *Public Attitudes About Eye and Vision Health.* JAMA Ophthalmology, 2016. **134**(10): p. 1111-1118.
4. Etten, P., *macular hole repair.* 2016.
5. Narendran, V. and A. Kothari, *Principles and Practice of Vitreoretinal Surgery.* 2014: JP Medical Ltd.
6. Shimozono, M., et al., *Three-step incision for 23-gauge vitrectomy reduces postoperative hypotony compared with an oblique incision.* Ophthalmic Surg Lasers Imaging, 2011. **42**(1): p. 20-5.
7. Matossian, C., S. Makari, and R. Potvin, *Cataract surgery and methods of wound closure: a review.* Clinical Ophthalmology (Auckland, NZ), 2015. **9**: p. 921.
8. Singh, A. and J.M. Stewart, *25-gauge sutureless vitrectomy: variations in incision architecture.* Retina (Philadelphia, Pa.), 2009. **29**(4): p. 451-5.
9. Spandau, U. and G. Scharioth, *Possible Surgeries After Insertion of a Trocar at Pars Plana*, in *Complications During and After Cataract Surgery*, U. Spandau and G. Scharioth, Editors. 2014, Springer Berlin Heidelberg: Berlin, Heidelberg. p. 155-183.
10. ECKARDT, C., *TRANSCONJUNCTIVAL SUTURELESS 23-GAUGE VITRECTOMY.* RETINA, 2005. **25**(2): p. 208-211.
11. Inoue, M., et al., *Two-step oblique incision during 25-gauge vitrectomy reduces incidence of postoperative hypotony.* Clin Exp Ophthalmol, 2007. **35**(8): p. 693-6.
12. Yeshurun, I., T. Rock, and E. Bartov, *Modified sutureless sclerotomies for pars plana vitrectomy.* American journal of ophthalmology, 2004. **138**(5): p. 866-7.
13. Klufas, M., *Trocar/Cannula Roundup.* New Retina MD, 2016.
14. Meyer, C., et al., *Geometry, penetration force, and cutting profile of different 23-gauge trocars systems for pars plana vitrectomy.* Retina (Philadelphia, Pa.), 2014. **34**.
15. Gupta, O.P., et al., *The Competency of Pars Plana Vitrectomy Incisions: A Comparative Histologic and Spectrophotometric Analysis.* American Journal of Ophthalmology, 2009. **147**(2): p. 243-250.e1.
16. Madanagopalan, V., et al., *Influence of orientation of the external linear incision created by the 25-gauge trocar and related factors on sclerotomy closure: A clinical and optical coherence tomographic study.* Indian journal of ophthalmology, 2018. **66**(12): p. 1809.
17. Eilaghi, A., et al., *Biaxial mechanical testing of human sclera.* Journal of Biomechanics, 2010. **43**(9): p. 1696-1701.
18. Shin, A., J. Park, and J.L. Demer, *Opto-mechanical characterization of sclera by polarization sensitive optical coherence tomography.* Journal of Biomechanics, 2018. **72**: p. 173-179.
19. Boote, C., et al., *Scleral structure and biomechanics.* Progress in Retinal and Eye Research, 2020. **74**: p. 100773.
20. Coudrillier, B., et al., *Collagen structure and mechanical properties of the human sclera: analysis for the effects of age.* Journal of biomechanical engineering, 2015. **137**(4).
21. Schultz, D.S., et al., *Structural Factors That Mediate Scleral Stiffness.* Investigative Ophthalmology & Visual Science, 2008. **49**(10): p. 4232-4236.
22. Friberg, T.R. and J.W. Lace, *A comparison of the elastic properties of human choroid and sclera.* Experimental Eye Research, 1988. **47**(3): p. 429-436.
23. Pinsky, P.M., D. van der Heide, and D. Chernyak, *Computational modeling of mechanical anisotropy in the*

cornea and sclera. Journal of Cataract & Refractive Surgery, 2005. **31**(1): p. 136-145.
24. Kelly, P., *Solid Mechanics.* Part I, Lecture notes, The University of Auckland. 2013.
25. Hibbeler, R., *Mechanics of Materials Eigth Editlion.* 2010: Pearson Education, Inc.
26. Han, S.F. and Y. Yang, *Influence of needling conditions on the corneal insertion force.* Computer Methods in Biomechanics and Biomedical Engineering, 2019. **22**(16): p. 1239-1246.
27. van Gerwen, D.J., J. Dankelman, and J.J. van den Dobbelsteen, *Needle–tissue interaction forces – A survey of experimental data.* Medical Engineering & Physics, 2012. **34**(6): p. 665-680.
28. Wu, P.-C., et al., *TWISTING MANEUVER FOR SUTURELESS VITRECTOMY TROCAR INSERTION TO REDUCE INTRAOPERATIVE INTRAOCULAR PRESSURE RISE.* RETINA, 2011. **31**(5).
29. Mahvash, M. and P.E. Dupont. *Fast needle insertion to minimize tissue deformation and damage.* in *2009 IEEE International Conference on Robotics and Automation.* 2009.
30. Lenau, T., et al., *Mosquito inspired medical needles.* SPIE Smart Structures and Materials + Nondestructive Evaluation and Health Monitoring. Vol. 10162. 2017: SPIE.
31. Sakes, A., D. Dodou, and P. Breedveld, *Buckling prevention strategies in nature as inspiration for improving percutaneous instruments: a review.* Bioinspiration & Biomimetics, 2016. **11**(2): p. 021001.
32. Lyimo, I.N. and H.M. Ferguson, *Ecological and evolutionary determinants of host species choice in mosquito vectors.* Trends in Parasitology, 2009. **25**(4): p. 189-196.
33. Matthews, A., et al., *Indentation and needle insertion properties of the human eye.* Eye, 2014. **28**(7): p. 880-887.
34. Pulido, J.S., M.E. Zobitz, and K.N. An, *Scleral penetration force requirements for commonly used intravitreal needles.* Eye, 2007. **21**(9): p. 1210-1211.
35. Thompson, J.T., *Advantages and Limitations of Small Gauge Vitrectomy.* Survey of Ophthalmology, 2011. **56**(2): p. 162-172.
36. Hsu, J., et al., *Hypotony After 25-Gauge Vitrectomy Using Oblique Versus Direct Cannula Insertions in Fluid-Filled Eyes.* RETINA, 2008. **28**(7).
37. Chen, J.C., *Sutureless Pars Plana Vitrectomy Through Self-sealing Sclerotomies.* Archives of Ophthalmology, 1996. **114**(10): p. 1273-1275.
38. Chen, D., et al., *Sutureless Vitrectomy Incision Architecture in the Immediate Postoperative Period Evaluated In Vivo Using Optical Coherence Tomography.* Ophthalmology, 2010. **117**(10): p. 2003-2009.
39. Singh, S.P.N. and C.N. Riviere. *Physiological tremor amplitude during retinal microsurgery.* in *Proceedings of the IEEE 28th Annual Northeast Bioengineering Conference (IEEE Cat. No.02CH37342).* 2002.
40. McDonnell, P.J., et al., *Dynamic morphology of clear corneal cataract incisions.* Ophthalmology, 2003. **110**(12): p. 2342-2348.
41. Taban, M., et al., *Dynamic morphology of sutureless cataract wounds—effect of incision angle and location.* Survey of Ophthalmology, 2004. **49**(2, Supplement 2): p. S62-S72.
42. Schaer, G.N., O.R. Koechli, and U. Haller, *Single-use versus reusable laparoscopic surgical instruments: A comparative cost analysis.* American Journal of Obstetrics and Gynecology, 1995. **173**(6): p. 1812-1815.
43. Siegel, G.W., et al., *Cost Analysis and Surgical Site Infection Rates in Total Knee Arthroplasty Comparing Traditional vs. Single-Use Instrumentation.* The Journal of Arthroplasty, 2015. **30**(12): p. 2271-2274.
44. Olsen, T.W., et al., *Human sclera: Thickness and surface area.* American Journal of Ophthalmology, 1998. **125**(2): p. 237-241.
45. Norman, R.E., et al., *Dimensions of the human sclera: Thickness measurement and regional changes with axial length.* Experimental Eye Research, 2010. **90**(2): p. 277-284.
46. Dalma-Weiszhausz, J., et al., *Intraocular pressure rise during 25-gauge vitrectomy trocar placement.* Graefe's Archive for Clinical and Experimental Ophthalmology, 2008. **246**(2): p. 187-189.
47. Shiose, Y., *Intraocular pressure: New perspectives.* Survey of Ophthalmology, 1990. **34**(6): p. 413-435.
48. Mital, A. and A. Kilbom, *Design, selection and use of hand tools to alleviate trauma of the upper extremities: Part II — The scientific basis (knowledge base) for the guide.* International Journal of Industrial Ergonomics, 1992. **10**(1): p. 7-21.
49. NASA, *HUMAN PERFORMANCE CAPABILITIES*, in *Man-System Integration Standards.* 1995.
50. Hanlon, M.a. and M. Laconte, *Trocar system having a drive.* 2019, Synergetics Inc.
51. Hanlon, M.a. and M. Laconte, *Trocar system having a drive.* 2014, Synergetics Inc.
52. Laconte, M.P., J.C. Easley, and J. Stroisch, *Surgical Devices with Triggered Propulsion System for Inserting a Trocar-Cannula Assembly.* 2018, Synergetics Usa Inc.
53. Chen, D.E., *Ophthalmic cannula insertion tool and method.* 2009, Medical Instr Dev Lab Inc.
54. Roberts, C. *Bausch + Lomb Shares Developments in Vitrectomy (OIS@ASRS 2016).* 2016.
55. Dvorak, E.M., et al., *Positioner for medical devices such as biopsy needles*, S. United, Editor. 2003, Wisconsin Alumni Research Foundation.
56. Hankins, C., *Apparatus and method for guiding a medical device in multiple planes*, S. United, Editor. 2007, Civco Medical Instruments Co Inc.
57. Scali, M., et al., *Needle-like instruments for steering through solid organs: A review of the scientific and patent literature.* Proceedings of the Institution of Mechanical Engineers, Part H: Journal of Engineering in Medicine, 2017. **231**(3): p. 250-265.
58. Glozman, D., et al., *Needle steering by shaft manipulation*, S. United, Editor. 2020, Technion Research and Development Foundation Ltd.
59. Yim, M., *Sharp turning steerable needle*, S. United, Editor. 2020, University of Pennsylvania Penn.
60. Alexander, G.G., Kathleen; Pollard, Alan; Pratt, David; Stocks, Susan, *Guidance on the administration to adults of oil-based depot and other long-acting intramuscular antipsychotic injections.* 2016.
61. Medtronic, *Medtronic Mio® Infusion Set User Guide.* 2012.
62. Fan, C., D. Dodou, and P. Breedveld, *Review of manual control methods for handheld maneuverable instruments.* Minimally Invasive Therapy & Allied Technologies, 2013. **22**(3): p. 127-135.
63. Teichgräber, C., J. Müglitz, and M. Berger. *Guiding Linkages with Remote Centre of Rotation for Thermal Cutting Processes.* in *Mechanisms, Transmissions and Applications.* 2018. Cham: Springer International Publishing.
64. Cuellar, J.S., et al., *Ten guidelines for the design of non-assembly mechanisms: The case of 3D-printed prosthetic hands.* Proceedings of the Institution of Mechanical Engineers, Part H: Journal of Engineering in Medicine, 2018. **232**(9): p. 962-971.
65. Culmone, C., et al., *Exploring non-assembly 3D printing for novel compliant surgical devices.* PLOS ONE, 2020. **15**(5): p. e0232952.

66. van Schoor, S., *Design of Non-Assembly Mechanisms for Desktop 3D*. 2020.
67. Hipps, J., et al., *Laser Eye Surgery Robot*. 2015.
68. Reilly, M., et al., *Simulations of Porcine Eye Exposure to Primary Blast Insult.* Optometry and Vision Science, 2015. **4**.
69. Larson, K., *Can You Estimate Modulus From Durometer Hardness for Silicones?* 2019.
70. May, W.N., et al., *Standardized Seidel test to evaluate different sutureless cataract incision configurations.* Journal of Cataract & Refractive Surgery, 2010. **36**(6): p. 1011-1017.
71. Dekking, F.M., et al., *A Modern Introduction to Probability and Statistics: Understanding why and how.* 2005: Springer Science & Business Media.
72. Zanaty, M., et al., *Programmable Multistable Mechanisms for Safe Surgical Puncturing.* Journal of Medical Devices, 2019. **13**(2).
73. Hopkins, J.B. and M.L. Culpepper, *Synthesis of multi-degree of freedom, parallel flexure system concepts via Freedom and Constraint Topology (FACT)–Part I: Principles.* Precision Engineering, 2010. **34**(2): p. 259-270.
74. Hopkins, J.B. and M.L. Culpepper, *Synthesis of multi-degree of freedom, parallel flexure system concepts via freedom and constraint topology (FACT). Part II: Practice.* Precision Engineering, 2010. **34**(2): p. 271-278.
75. Hricko, J. and Š. Havlík. *Compliant mechanisms for motion/force amplifiers for robotics.* in *International Conference on Robotics in Alpe-Adria Danube Region.* 2019. Springer.
76. Van Boeijen, A., et al., *Delft design guide: Design strategies and methods.* 2014.
77. Sakes, A., et al., *Shooting Mechanisms in Nature: A Systematic Review.* PLoS One, 2016. **11**(7): p. e0158277.
78. Schwenk, K. and D.A. Bell, *A cryptic intermediate in the evolution of chameleon tongue projection.* Experientia, 1988. **44**(8): p. 697-700.
79. Brau, F., et al., *Dynamics of prey prehension by chameleons through viscous adhesion.* Nature Physics, 2016. **12**(10): p. 931-935.
80. Anderson, C.V., *Off like a shot: scaling of ballistic tongue projection reveals extremely high performance in small chameleons.* Sci Rep, 2016. **6**: p. 18625.
81. Anderson, C.V. and S.M. Deban, *Thermal effects on motor control and in vitro muscle dynamics of the ballistic tongue apparatus in chameleons.* J Exp Biol, 2012. **215**(Pt 24): p. 4345-57.
82. Anderson, C.V. and S.M. Deban, *Ballistic tongue projection in chameleons maintains high performance at low temperature.* Proc Natl Acad Sci U S A, 2010. **107**(12): p. 5495-9.
83. Anderson, C.V., N.P. Larghi, and S.M. Deban, *Thermal effects on the performance, motor control and muscle dynamics of ballistic feeding in the salamander Eurycea guttolineata.* J Exp Biol, 2014. **217**(Pt 17): p. 3146-58.
84. Deban, S.M., et al., *Evolution of a high-performance and functionally robust musculoskeletal system in salamanders.* Proceedings of the National Academy of Sciences, 2020. **117**(19): p. 10445-10454.
85. Dumeril, *Erpetologie generale: ou, Histoire naturelle complete des reptiles.* 1836.
86. Houston, J., *On the structure and mechanism of the tongue of the chameleon.* The Transactions of the Royal Irish Academy, 1828: p. 177-201.
87. Brücke, E., *Über die Zunge der Chamäleonen.* Sitzungsberichte der Mathematisch-Naturwissenschaftlichen Classe der Kaiserlichen Akademie der Wissenschaften, 1852. **8**: p. 65-70.
88. Gnanamuthu, C. *27. The Anatomy and Mechanism of the Tongue of Chamadeon carcaratus (Merrem).* in *Proceedings of the Zoological Society of London.* 1930. Wiley Online Library.
89. Gnanamuthu, C. *Comparative study of the hyoid and tongue of some typical genera of reptiles.* in *Proceedings of the Zoological Society of London.* 1937. Wiley Online Library.
90. Zoond, A., *THE MECHANISM OF PROJECTION OF THE CHAMELEON'S TONGUE.* 1933.
91. WAINWRIGHT, P.B., A, *THE MECHANISM OF TONGUE PROJECTION IN CHAMELEONS I.* 1992.
92. WAINWRIGHT, P.B., A, *THE MECHANISM OF TONGUE PROJECTION IN CHAMELEONS II.* 1992.
93. de Groot, J.H. and J.L. van Leeuwen, *Evidence for an elastic projection mechanism in the chameleon tongue.* Proc Biol Sci, 2004. **271**(1540): p. 761-70.
94. Moulton, D.E., et al., *The elastic secrets of the chameleon tongue.* Proceedings of the Royal Society A: Mathematical, Physical and Engineering Sciences, 2016. **472**(2188).
95. Van Leeuwen, J., *Why the chameleon has spiral-shaped muscle fibres in its tongue.* 1997: p. 573–589.
96. Kier, W.M., *The diversity of hydrostatic skeletons.* J Exp Biol, 2012. **215**(Pt 8): p. 1247-57.
97. Deban, S.M. and U. Dicke, *Activation patterns of the tongue-projector muscle during feeding in the imperial cave salamander Hydromantes imperialis.* J Exp Biol, 2004. **207**(Pt 12): p. 2071-81.
98. Scales, J., S.V. Bloom, and S.M. Deban, *Convergently evolved muscle architecture enables high-performance ballistic movement in salamanders.* J Morphol, 2020. **281**(2): p. 196-212.
99. Lu, Z., *A Catapult Robot with Chameleon-inspired MultiBody Elastic Nested System.* 2017.
100. Zheng, Z.W., K; Wu, X; Zhang, Q; Li, K, *Dynamic Analysis of Elastic Projecting Robot inspired by Chameleon Tongue.* 2018.
101. Debray, A., *Manipulators inspired by the tongue of the chameleon.* Bioinspir Biomim, 2011. **6**(2): p. 026002.

Appendices

A. Interviews with Surgeons

Peter van Etten

Context

(27 November 2020) The project started with the idea that fast insertion of a trocar could lower the pressure in the eye during insertion and by doing so reduce complications. This first interview with Peter van Etten, a surgeon at the Retina Operatie Centrum Utrecht (ROCU), and was meant as an early explorative interview to design a tool that surgeons would want.

Q: Have you ever encountered the pressure in the eye to a problem

A: There are some cases where it could result in problems, for instance in the case of open eye trauma, in these cases the trocar cannot be used, and the incision is made with a stiletto blade instead. However, in the surgeries where the trocar is used there are other steps in the surgery that cause a lot more deformation and pressure increase. One of these steps is scleral buckling, where the eye is severely deformed, and this does not result in permanent damage. It likely that the effect of pressure increase of trocar insertion is neglectable compared to these other forces.

Q: What is important during the surgery

A: The creation of a nice non leaking tunneled incision is the most important. During insertion of the trocar, you try to create a path that seals itself under the ocular pressure and prevents fluids from inside the eye from leaking out. The angle of insertion is very important in the creation of well sealing steps in the tunnel.

Q: what mistakes do inexperienced doctors make

A: Young surgeons run the risk of overshooting and hitting other structures and damaging them. The insertion should be limbus parallel (facing the iris in the tangential direction) to minimize this risk. It requires some getting used to handling the eye. It also takes some practice to insert some cannulas depending on right or left handedness.

Q: How long does the surgery take and what would be an acceptable added time for reduced complications.

A: The macular hole repair shown in the YouTube video [4] takes around 45-60min, the insertion of the cannulas is the first few minutes. A new device should not take much longer to insert as time in the OR is expensive, however the decision on what would be acceptable is difficult to make without knowing the improvement in complications.

Niels Crama and Sander Keijser

Context

(29 December 2020) The interview with van Etten lead to a shift in view on the goal of the thesis. A second surgeon was found. Niels Crama and Sander Keijser are eye surgeons at the Radboud university medical center in Nijmegen. The questions go into the incision style they use.

Q: What incision style are you aiming for?

A: We are trying to create a little bend halfway the tunnel. It is interesting to look at the incisions from a mechanical perspective, as most of the incisions are made based on expertise. We haven't thought about the incisions in this way. We would like to go a planar as possible to limit leakage and lengthen the tunnel preventing ingress of microbes. The length on which the tool is inserted is easy, however the depth feedback is limited and therefor difficult to gauge. The depth is important for the moment of canting the blade. I explicitly call it canting and not turning as the tool should rotate around the tip and not just be turned as a whole. We do not know the exact effect but maybe a rough tunnel surface might create a better sealing wound as opposed to a perfectly clean one. The sclera is quite elastic and deforms when the tool is inserted, you have to account for this. The elasticity also changes with age, where younger sclera up to the age of 40 are more flexible. This is not in favor of the patient as older, stiffer sclera seal better. When looking at tri-planar incision you should also look at cataract surgery as more elaborate incision architecture are used. The incisions are little bit easier to make as the cornea is clear and you can clearly see what you are doing.

Q: What is the effect of gauge size?

A: Smaller incisions have a positive effect on the leaking and healing of the eye. The effect is already very noticeable as we switch from 20 Gauge to 23 Gauge. The current stiffness of surgical equipment is the main limiting factor why we cannot go smaller. The current optimum for us is at 23 Gauge tools as we encounter less complications and still have the benefit of the stiffer tooling. In the future the tools might develop and then this tradeoff will change in favor of smaller gauge sizes.

Q: Are there differences between trocars?

A: Geometry of the blade, for instance stiletto or beveled blades, make quite a bit of difference on how well the trocar cuts through the sclera. There have been quite some improvements in the last few years, and I hope this trend will continue.

Q: in a aided tool, what should the surgeon absolutely do himself

A: The choice of location of the tool should absolutely be done by the surgeon himself. Apart from that, if the tool would perform a better incision than I could do by hand everything is fine. This could mean just placing tool on the eye and pressing a button and it placing the cannula.

Q: what velocity are you aiming for

A: We are not aiming for a specific velocity. There has been research in velocity, however that is only clinically relevant in open eye trauma. In an open eye trauma the eye gives to little counterpressure for insertion of the trocar and there is a risk of further propagation of the trauma.

B. Stakeholder Analysis

Implementation of a new surgical tool has several stakeholders. In this appendix the wishes of the stakeholders in a future product are summarized.

Patient

The patient wishes the lowest risk of complications, the cost doesn't play a role as they are not the one paying. The patient would have very limited interactions with the device itself and likely will never see it in person.

Manufacturer (e.g. DORC)

The manufacturer will be the designer and producer of the tool. The main goal will be to make a profit from the device they will be producing. The market for trocars is highly competitive and currently, as there is very limited innovation the main competing factor is cost. Most research is focused on improvement of current designs, in the form of sharper blades, stiffer instruments and improved production techniques. The manufacturer is willing to innovate as new innovations lead to increased publicity, however, they should be proven first before they can be used in the field. (Mart Gahler, DORC)

Insurance

The insurance is the party that eventually pays the cost of the device. The main drive is to keep the total cost of the surgery down, however this includes the cost of complications. The insurance is more likely to include the new technique if it is cheaper including the cost of complications. If the insurance does not cover the cost the adoption will be hampered.

The main challenge between the wishes of the different stakeholders seems to be between the total cost of surgery and the risk of complications. The aim for this tool is to reduce the risk of complications using the new method of a tri-planar incision and design for a minimal cost. However, as the development is currently in a very early stage this deliberation based on cost should be covered at a later stage in development.

Surgeon

Surgeons are the ones using the device, but are also under pressure from multiple other parties, such as patients and the hospital. They wish a device is easy to use and consistent. Generally, surgeons like to have control over what is happening, a device should only add features they are not able to do themselves, be it in the form of speed or precision. For their patients they a lower risk of complications for a better doctor patient relationship, but also due to time savings in treating the complications. The hospital will apply pressure to keep cost down and put strict time and material budgets on the surgeons, therefor a lower cost and lower surgical time would improve the adoption.

A device that would satisfy the surgeon would have a similar functional structure as depicted in Figure 48. The mechanism is placed in the desired location on the sclera and activated, creating the perfect incision.

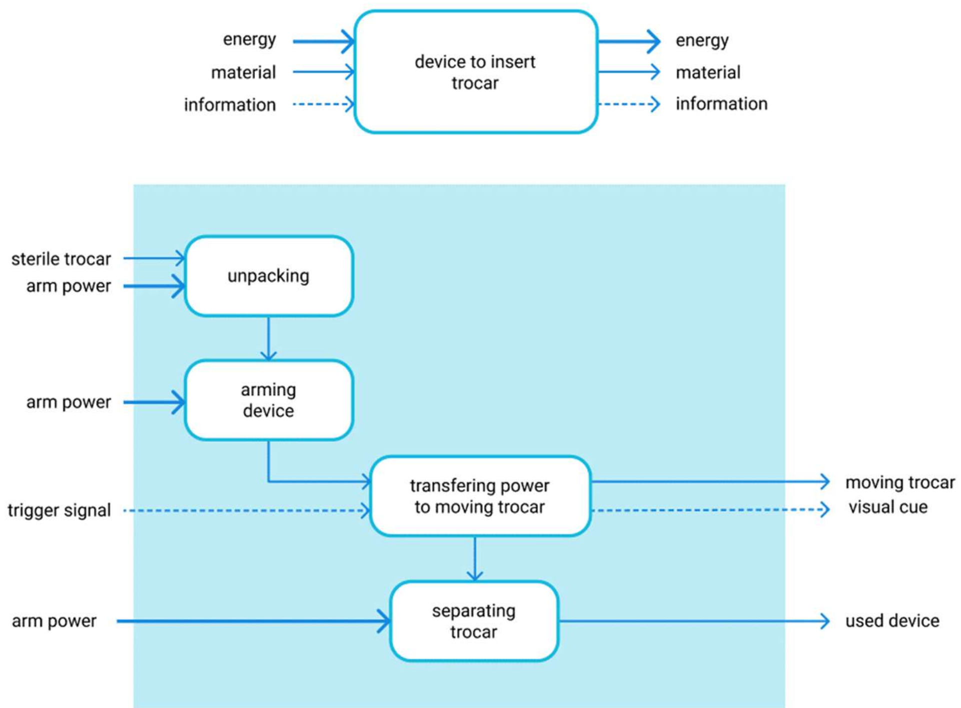

Figure 48: possible functional structure as envisioned by surgeon.

C. Decision-aid Depth Guidance

This appendix aims to aid in the decision of the depth guidance mechanisms. It will start with some slight detailing of how the mechanisms would work, using kinematic models made in LEGO. It will end with a comparison and decision between the two concept subsystems.

Pantograph Mechanism

The first mechanism is the pantograph mechanism. The desired reduction ratio and resulting mechanical is achieved using similar triangles in the linked connections. The origin of the scaling should close to the insertion location for precise movement. Therefor ideally the input and output would be on the same side of the origin. There is a large variation of pantograph mechanism that would suffice. Several different versions were made using LEGO depicted in Figure 49.

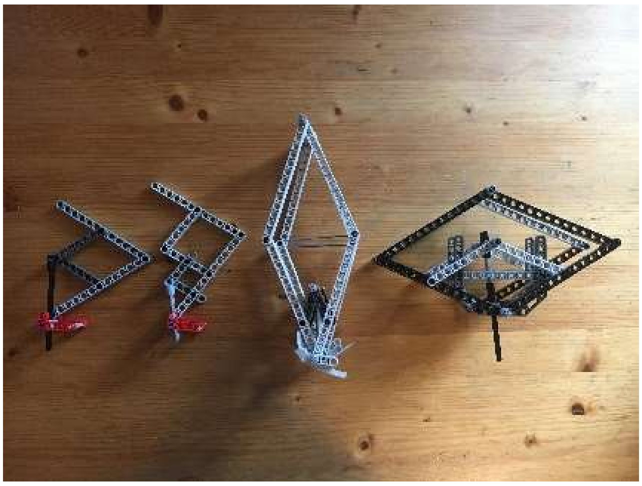

Figure 49: Pantograph mechanisms build in LEGO.

Screw Mechanism

The second mechanism is a screw mechanism. It uses the angled surface of the thread for mechanical advantage. If metric thread is chosen it can also be chosen to be self-locking, preventing it from unscrewing when pressure is applied on the tip of the trocar. The mechanism can reach very high reduction ratios.

The kinematics alone are not enough for an equal comparison, as an extra subsystem is necessary to prevent rotation of the trocar. Using the FACT method [73, 74] and inspiration from *Hricko et al* [75], several options for guidance were derive. Leaf flexures were concluded to be the simplest option and were selected for this design. The maximum deflection of these type of flexures in a 3D printed product were advised by MTB3d, a company specialized in 3d printing in Delft, to be a maximum of around 15°. To reach the required deflection the flexures should be around 30mm in length minimum. A first test of the screw mechanism was made using LEGO as depicted in Figure 50.

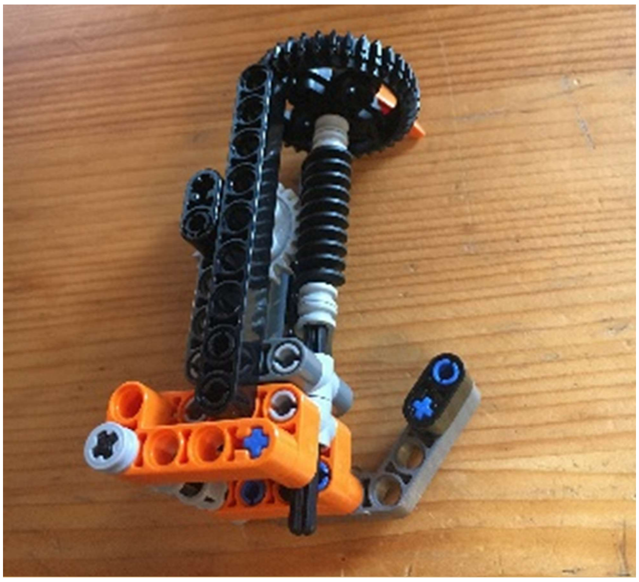

Figure 50: Screw mechanism build in LEGO.

Comparison and Decision

To aid in the choice between the two options a Harris profile was used from the Delft Design Guide [76]. The Harris profile is a tool to visualize the reasons behind a decision and through that aiding in ordering the pros and cons of a certain design, as depicted in Figure 51. For the sub-system on depth guidance the decision must be made between a pantograph and a screw mechanism. The evaluation criteria on the left of the Harris diagram are a simplified reformulation of the criteria from the requirements, the bar on the right visualizes a relative score to other concepts. The importance of the criteria is ordered from important to less important.

The pantograph mechanism scores well, however not so on the repeatability and size of the mechanism. These two points require a lot of work to meet the requirements. Unfortunately, these are also the two most important factors in the decision of the design. The screw mechanism scores very well on these points, but requires some work to lower the insertion time in a future iteration.

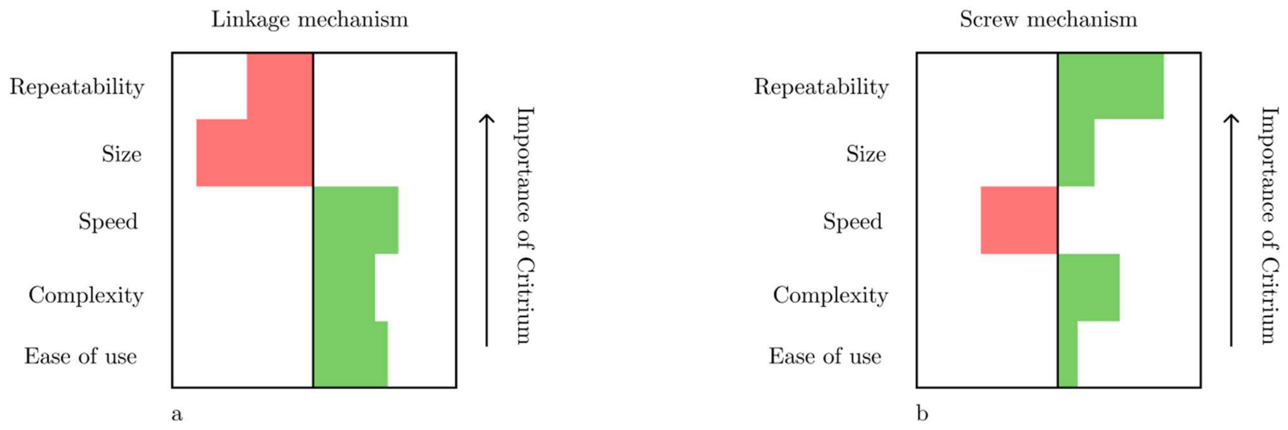

Figure 51: Harris diagram of two possible solutions for depth guidance. a) Harris Diagram pantograph mechanism b) Harris Diagram Screw mechanism.

D. Chameleon and Salamander Tongue Shooting

In case a high velocity is required there are plenty of examples in nature. Looking for a combination of guiding and velocity there are many examples [77]. A striking example is the tongue shooting mechanism in a chameleon. It is, light weight, highly repeatable and precise. Combination of high velocity and guiding would enable the creation of a novel medical instrument.

Chamaeleonid, iguanid and agamid lizard use their tongue to capture prey in the form of locusts and other insects and are evolutionary closely related [78]. Where other lizards use the jaws for prey prehension, these species have evolved rapid tongue firing mechanisms that are able to launch the tongue forward and stick to the prey due to viscous adhesion [79]. The mechanism for the Chameleon and Plethodontid salamanders (lungless salamander) are highly specialized and able to reach extreme accelerations. The maximum acceleration reported in literature is 264g, observed in the Rhampholeon spinosus [77]. The Plethodontid salamanders tongue is able to reach even higher accelerations of up to 458g in Bolitoglossa dofleini [80]. The tongue can reach this performance relatively independent from temperature, which is crucial for ectothermic animals[81-84]. Both animals use elastic collagen tissue to store energy for launch to be able to reach these high velocities, but use slightly different mechanisms as is elaborated below. Evolution is working towards an ideal solution, in a race of survival of the fittest. It may generate highly specialized solutions for the species to gain an advantage to reproduce. Natural mechanism can function as perfect sources of inspiration for novel new mechanisms.

Chameleon Tongue Shooting Mechanism

The prey prehension in chameleons consist of three phases four parts: Fixation on prey and protrusion of the hypoid bone, Contraction of the launching muscles resulting ballistic phase of the tongue and finally retraction with the prey. The chameleon tongue has been a subject of research, in the early 19th century it was thought that the tongue was launched using rapid filling of the tongue with air [85] from the lungs or blood [86]. Later, these theories were rejected by morphological works [87-90], which concluded the tongue is indeed launched using muscles in the tongue. This was expanded on this by examining the activation of the muscles and the launching mechanism [91, 92].

The tongue of a bone, the epiglossal process, surrounded by a sheet of helically wound collagen fibers and covered by a cylindrical accelerator muscle. The current understanding is that the energy is stored in the elastic collagen due to deformation of the accelerator muscle [93, 94]. This energy is released when the accelerator muscle is launched from this long cylindrical bone. When the muscle contracts this leads to an inward normal force and deformation of the accelerator muscle. The accelerator muscle of the tongue will work like a muscular hydrostat, retaining a constant volume, like the tentacles of a squid [95, 96]. Muscle fibers are oriented in radial spirals, when these are contracted will cause the accelerator muscle become thinner and to elongate along the epiglossal bone [93]. When reaching the end of the process a longitudinal normal force will appear causing the tongue to accelerate. No separate trigger mechanism is necessary as the contraction of the accelerator muscle will trigger itself when the end of the bone is reached. The mechanism works similar to a melon seed squeezed between fingers. The working principle is depicted in Figure 52.

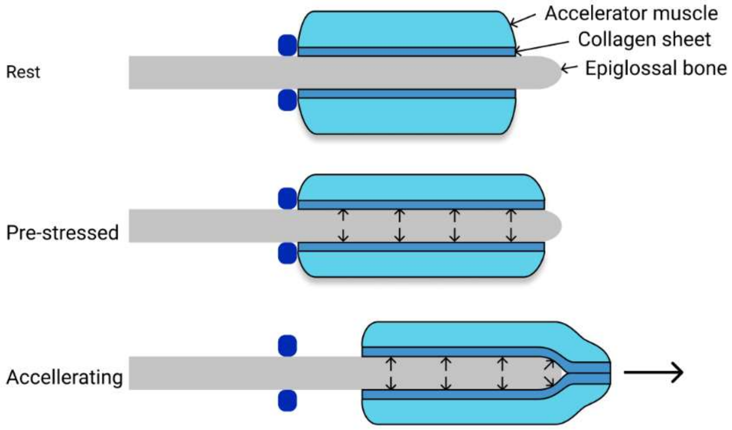

Figure 52: Working mechanism chameleon tongue based on [93].

Lungless Salamanders Tongue Shooting Mechanism

Even though the species are quite evolutionary closely related, the biomechanical constructions in the tongue use different approaches and evolved in parallel [78]. Both use a muscle powered squeeze catapult mechanism which might be considered as the inverse version of one another [77]. In chameleons the hyobranchial apparatus remains in the mouth and the tongue protractor muscle is propelled at the prey, in plethodontidae a bone is accelerated and the muscles will remain in the mouth.

The basibranchial, also known are the tongue bone, is tapered along the length around which the subarcualis retis (SAR) lies, the lizard equivalent of the accelerator muscle [97]. The morphology of the bones and muscles is depicted in Figure 53. Due to the taper of the bone a component of the normal force will parallel to the surface and accelerate the bone. This mechanism evolved from the non-ballistic tongue found in other salamanders to a ballistic tongue using elastic energy storage and increased performance [84, 98]. The taper enables the use short sarcomeres that can generate high force low velocity and transfer that to low force high velocity. This effect is exaggerated by the medial folding of the tongue skeleton, which thrusts the basibranchial and the attached tongue pad forward faster than the epibranchial moves. [97] The animal is still able to modulate the exit velocity at lower velocities and rarely overshoots. [97] In the chameleon the launching is initiated by the shape change of the accelerator muscle causing the muscle to slide of the bone reaching the tapered tip. No such mechanism exist in Plethodontidae as the basibranchial is tapered along its full length and a forward force will be present when the muscles contract. To enable the accumulation of energy the bone passes a sphincter smaller than the one. Pressure builds up until buckling occurs in the medial folding, the bone can pass though and elastic energy from the muscle is released. This mechanism is schematically depicted in Figure 54.

To obtain more insight in the nature of the mechanism Arend Schot was contacted, a professor at the faculty of vetenary medicine of Utrecht, specialised at conservation of specimens. He was very helpful and allowed a visit the faculty to take a closer look at the mechanism in an actual chameleon. Unfortunately the faculty closed due to the corona measures in the netherlands and the meeting was cancelled. It remained an online conversation.

From Biology to Technology

The current state of the art of mechanism that use a similar principle is as follows. Tries to mimic this mechanism have already been made, however they do not resemble the biological mechanism very well. Concentric nested springs were used for energy storage [99, 100] or used a coil-gun and capacitor bank to mimic the accelerator [101]. Neither is able to reproduce the fascinating actuation principle of the chameleon tongue, nor the sliding due to a radially applied force by the muscular hydrostat. No mechanical equivalents have been found in literature for the plethodontid.

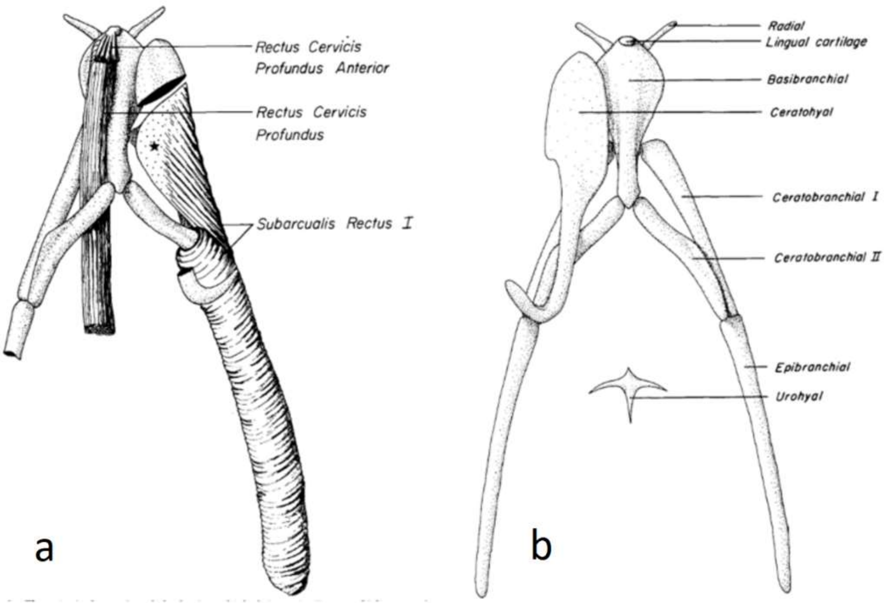

Figure 53: Morphology of a salamander tongue a) muscles inside the Plethodontid tongue [85] b) bones inside the Plethodontid tongue [85].

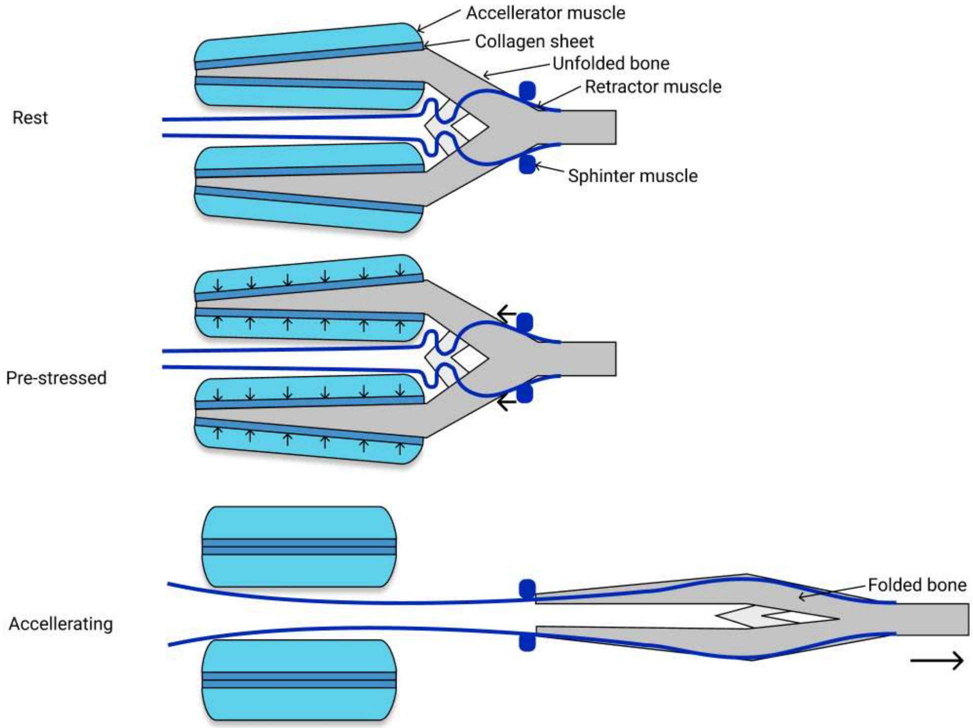

Figure 54: Working mechanism lizard tongue based on Sakes et al [77].

E. Experimental Results

Results: Flat Test

Three different experiments have been performed on flat silicone. The first test was on 0.5mm thick material, using India ink to stain the path. None of the incisions showed a tri-planar structure. More care was taken in the alignment of the trocar tip with the surface in the following test. The experiments were restarted with 2.0mm thick material and 0,5mm thick material. The incisions in these new tests did show a tri-planar structure. The incisions were trace from the microscopic images in a vector drawing software package called Figma and measured. The measurements of the incisions can be found in Table 7 and Table 8.

Thickness 0.5mm V1

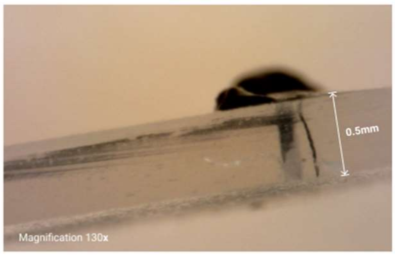

Test 1.1

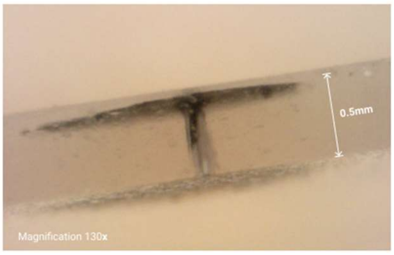

Test 1.2

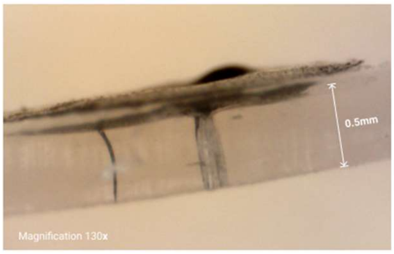

Test 1.3

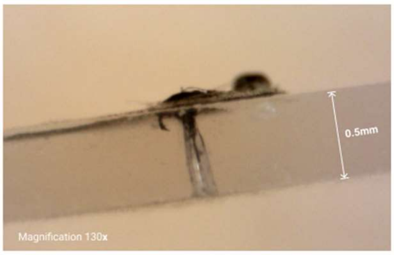

Test 1.4

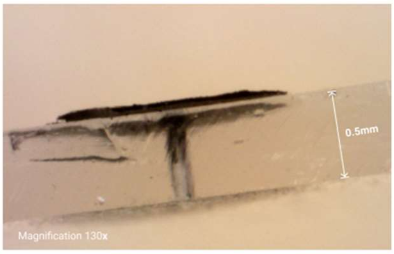

Test 1.5

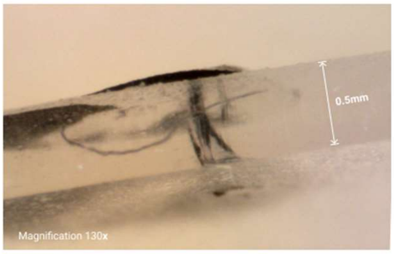

Test 1.6

Thickness 2.0mm

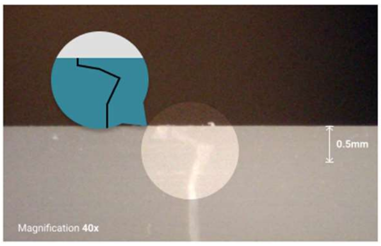

Test 2.1

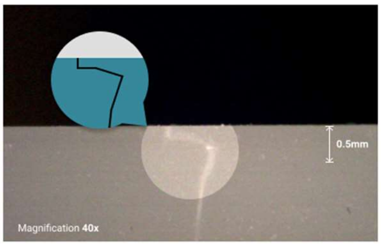

Test 2.2

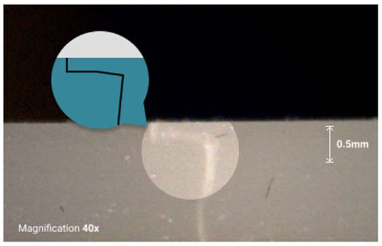

Test 2.3

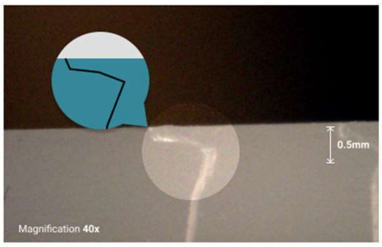

Test 2.4

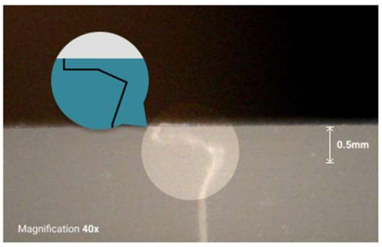

Test 2.5

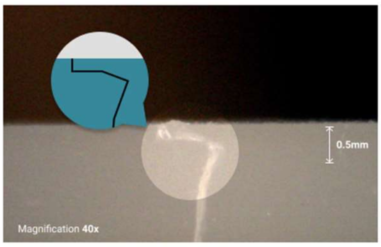

Test 2.6

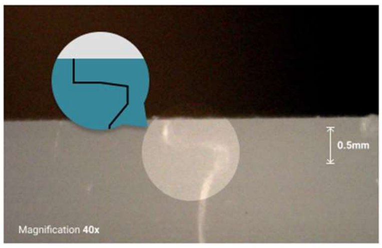

Test 2.7

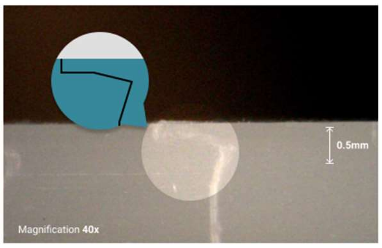

Test 2.8

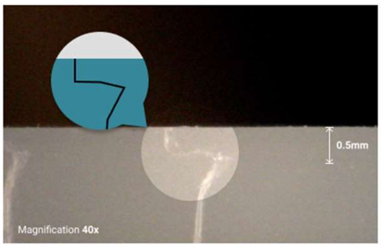

Test 2.9

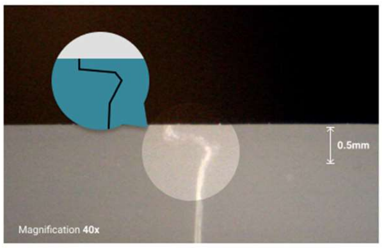

Test 2.10

Table 7: Results measurement of incisions in 2.0mm

Sample	Depth (mm)	Angle (°)	Length middle plane (mm)
2.1	0,10	72,90	0,60
2.2	0,14	79,49	0,62
2.3	0,19	86,25	0,76
2.4	0,14	76,65	0,76
2.5	0,15	78,37	0,87
2.6	0,18	80,15	0,77
2.7	0,33	86,09	0,73
2.8	0,19	82,55	0,96
2.9	0,31	83,07	0,67
2.10	0,14	75,38	0,59
avg	0,19	80,09	0,73
std	0,05	3,53	0,09

Thickness 0.5mm V2

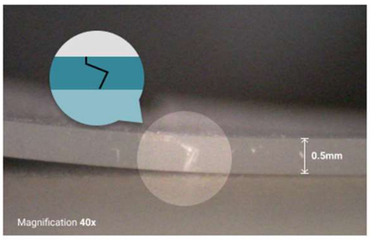

Test 3.1

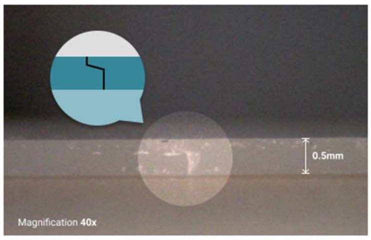

Test 3.2

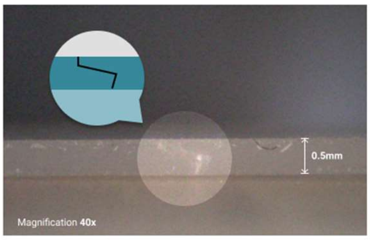

Test 3.3

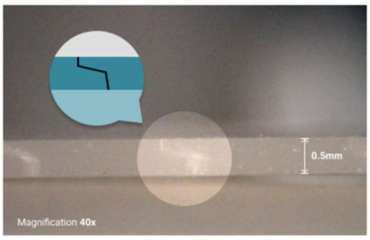

Test 3.4

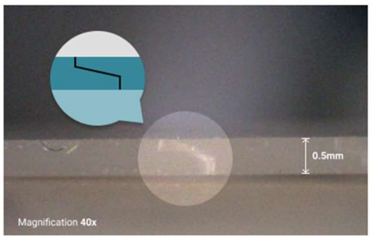

Test 3.5

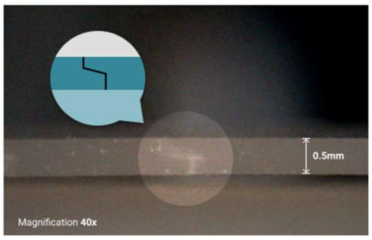

Test 3.6

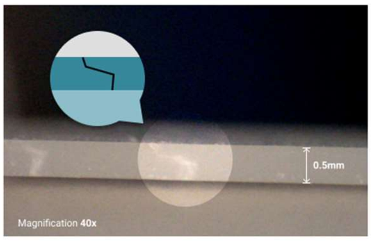

Test 3.7

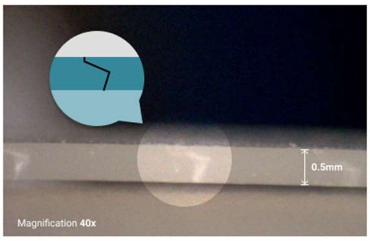

Test 3.8

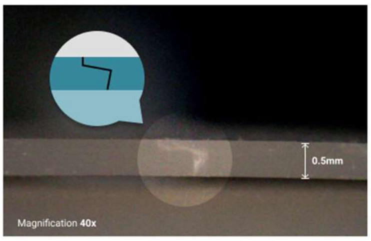

Test 3.9

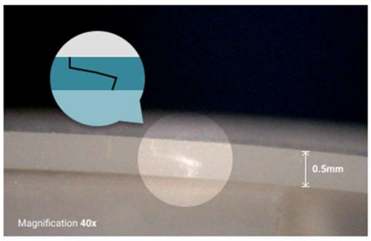

Test 3.10

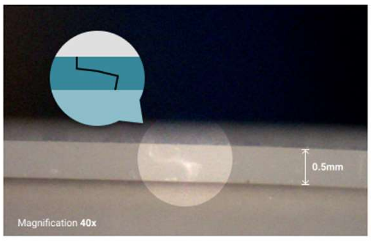

Test 3.11

Table 8: Results measurement of incisions in 0.5mm

Sample	Depth (mm)	Angle (°)	Length middle plane (mm)
3.1	0,10	68,40	0,32
3.2	0,12	75,00	0,25
3.3	0,13	77,40	0,54
3.4	0,13	77,21	0,40
3.5	0,14	77,59	0,64
3.6	0,16	75,43	0,32
3.7	0,13	74,02	0,40
3.8	0,06	66,80	0,38
3.9	0,12	79,66	0,40
3.10	0,15	77,58	0,67
3.11	0,17	79,87	0,58
avg	0,13	75,36	0,45
std	0,02	3,13	0,12

Results: Phantom Test

The test on the eye phantom consists of two parts. First the leakage of the incisions was measured and secondly the phantom was dissected, and the incision was analyzed. The leakage was measured from the droplet diameter on the microscope image. The measured diameter and calculated volume can be found in Table 9. The corresponding microscopic images of the incisions can be found below.

Leakage

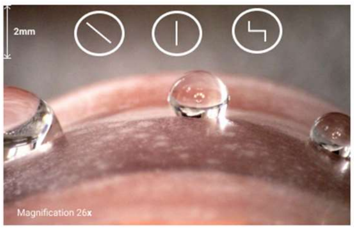

Test 5.1

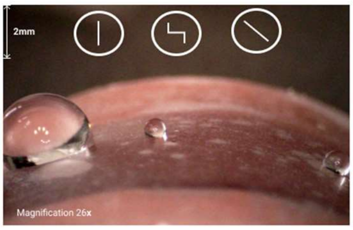

Test 5.2

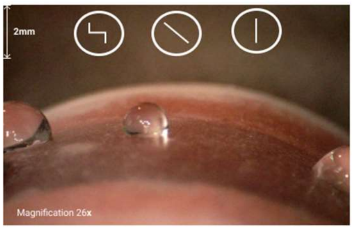

Test 5.3

Table 9: Droplet diameter and calculated leakage

[mm]	straight	oblique	tri-planar
Phantom 1	2,25	4,04	1,88
Phantom 2	3,31	0,98	0,65
Phantom 3	3,22	1,64	2,71

[µl]	straight	oblique	tri-planar
Phantom 1	5,96	34,53	3,48
Phantom 2	18,99	0,49	0,14
Phantom 3	17,48	2,31	10,42

Incision

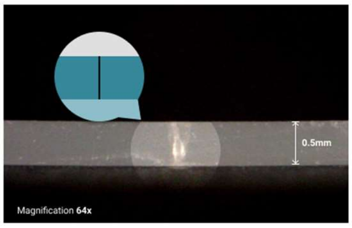

Test 4.1

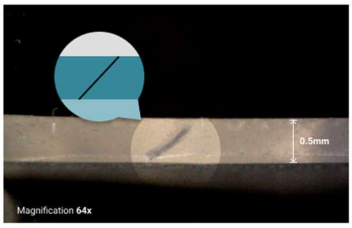

Test 4.2

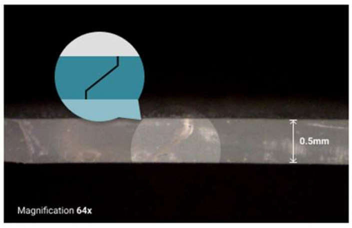

Test 4.3

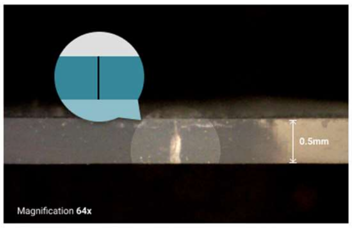

Test 4.4

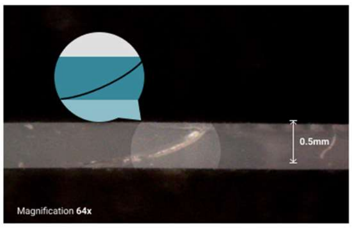

Test 4.5

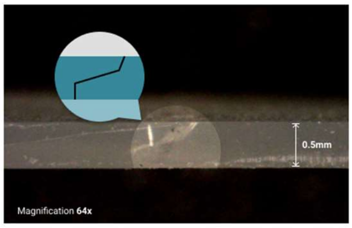

Test 4.6

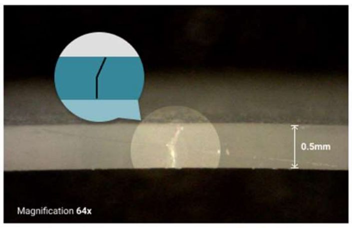

Test 4.7

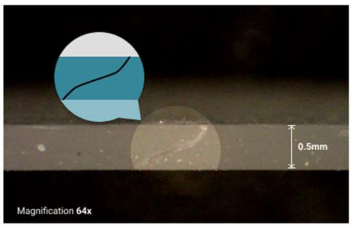

Test 4.8

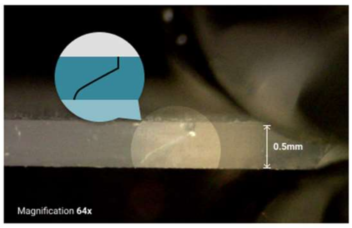

Test 4.9

Results: Wet Lab Test

The final test was on the ex-vivo porcine eyes. The fluid inside the eye was stained using India ink and the flow through the incision was observed. The incisions were ranked based on the visual flow of which the results can be found in Table 10. The images of the eyes are depicted below. The flow is difficult to observe in a static image, therefor the clips are available by contacting the author.

Leakage

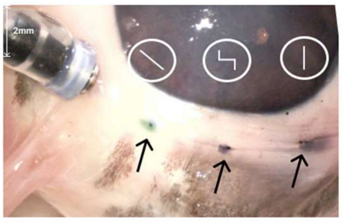

Test 6.1

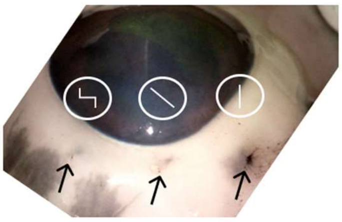
Test 6.2

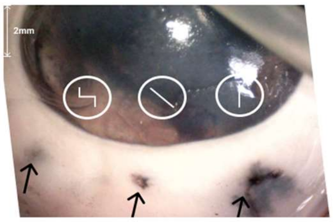

Test 6.3

Table 10: Table 11: Ranked performance of incisions in ex-vivo porcine eyes going from lowest leakage to highest, based on visual ink egress from the incision under the microscope.

	1.	2.	3.	Remarks
Phantom 1	Oblique	Tri-planar	Straight	Very little leakage on all incisions
Phantom 2	Tri-planar	Oblique	Straight	
Phantom 3	Oblique	Tri-planar	Straight	

F. Technical Drawings

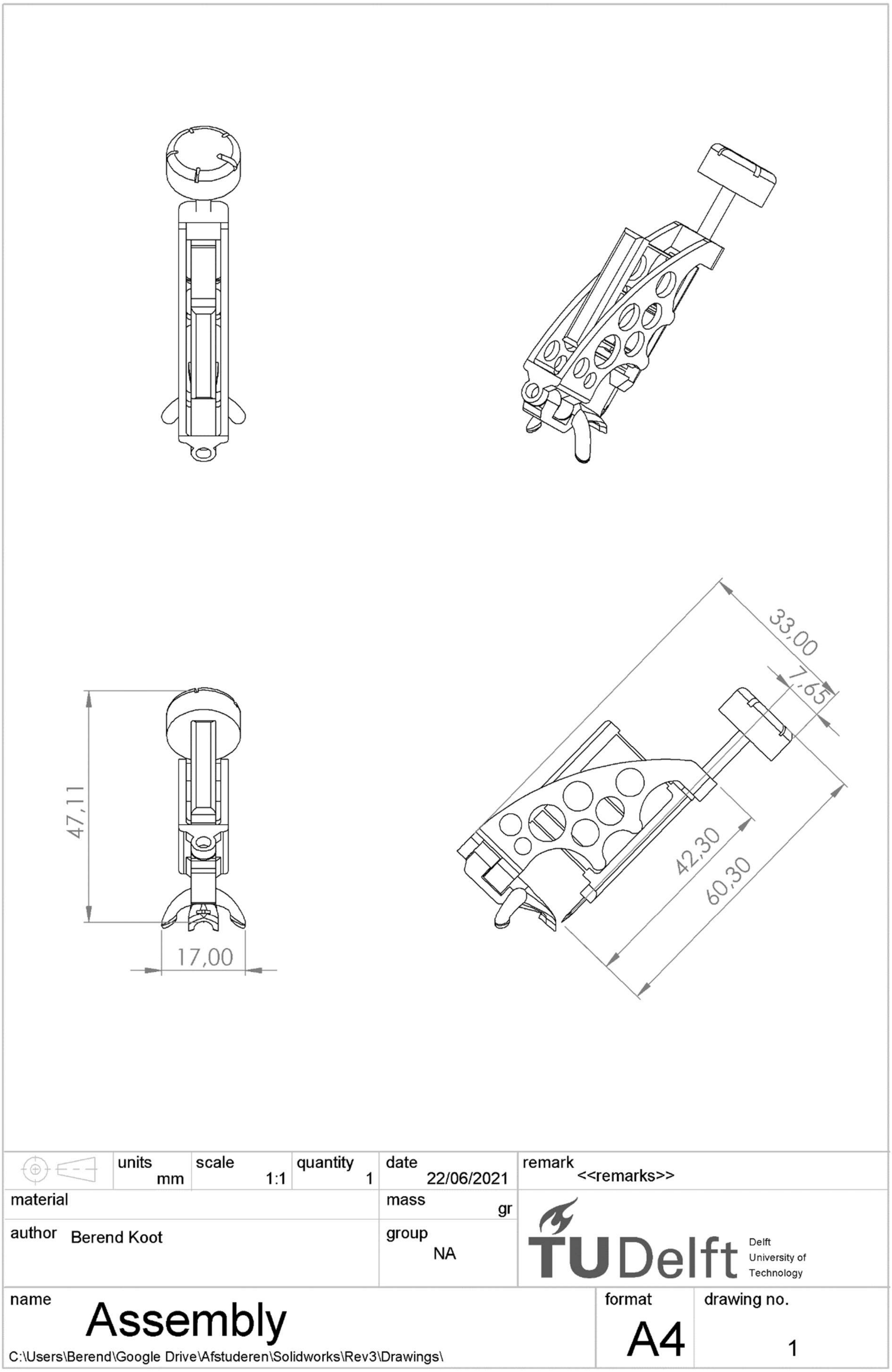

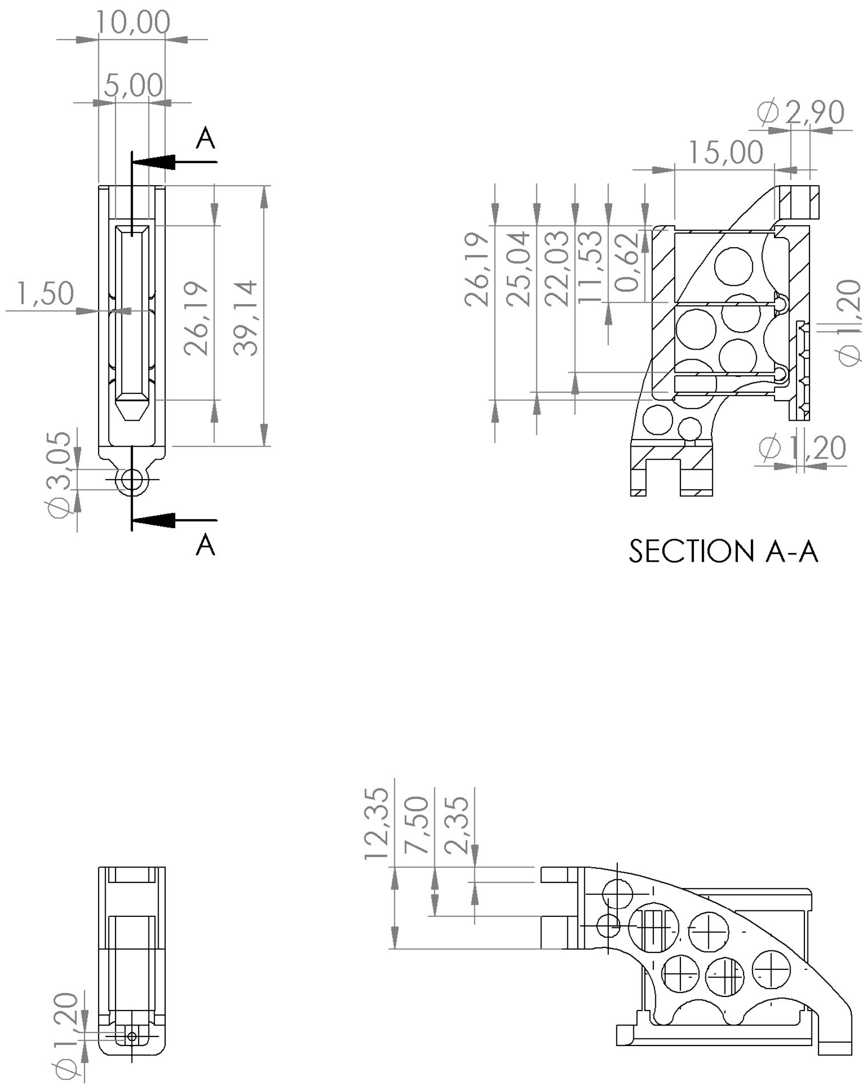

	units	scale	quantity	date	remark
	mm	1:1	1	22/06/2021	<<remarks>>

material

mass gr

author Berend Koot

group NA

TU Delft — Delft University of Technology

name **Screw Mechanism**

C:\Users\Berend\Google Drive\Afstuderen\Solidworks\Rev3\Drawings\

format A4

drawing no. 2

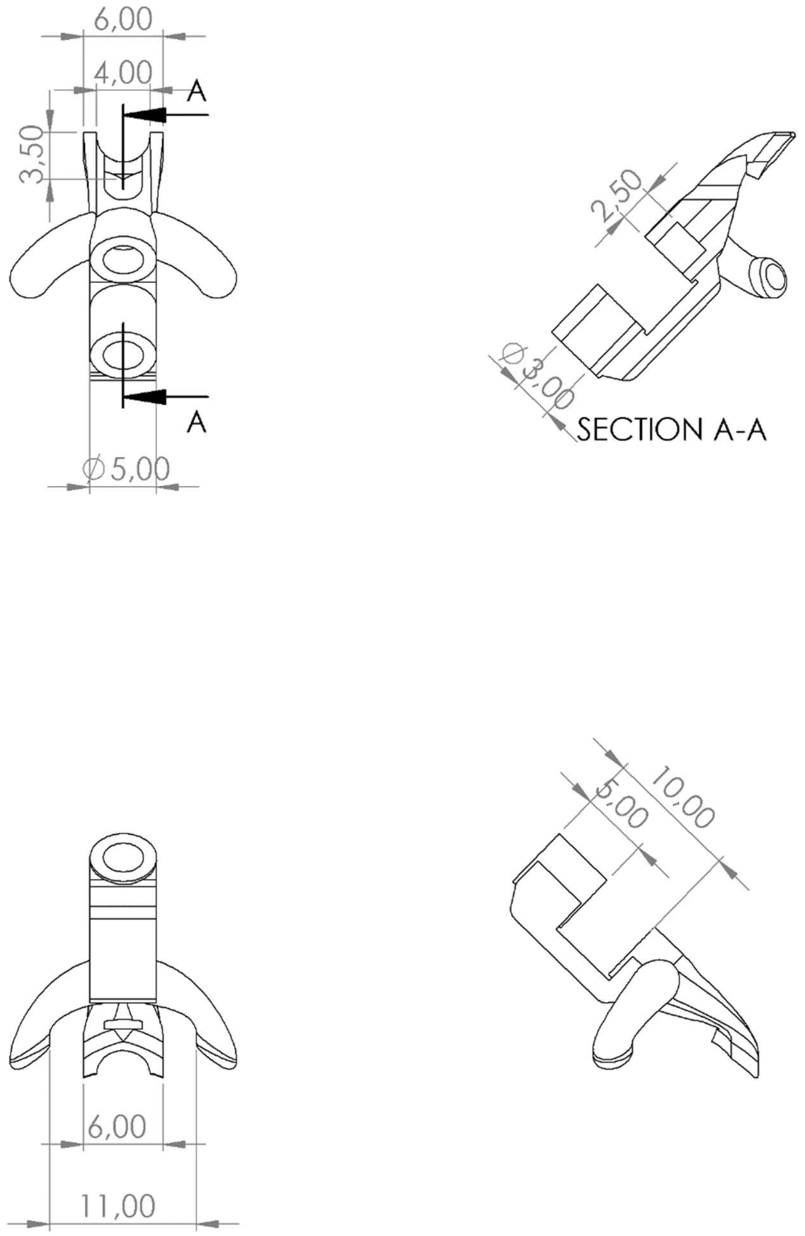

units mm	scale 2:1	quantity 1	date 22/06/2021	remark <<remarks>>
material			mass gr	TU Delft Delft University of Technology
author Berend Koot			group NA	
name **Ocular Reference**			format A4	drawing no. 3

C:\Users\Berend\Google Drive\Afstuderen\Solidworks\Rev3\Drawings\

G. Glossary

- Cannula – a tubular section that is placed in the sclera to allow the passage of instruments.
- DOF – degrees of freedom.
- Endophthalmitis – inflammation of the inside of the eye.
- Eye phantom – an artificial replica of a biological eye.
- Hypotony – low pressure inside the eye.
- IOP – intraocular pressure.
- OCT – optical coherence microscopy.
- Pars plana – the preferred anatomical area for the insertion of medical instruments in the eye.
- Sclera – the white part visible on the outside of the human eye.
- Sclerotomy – an incision in the sclera.
- Self-sealing – sealing without sutures instigated by the IOP.
- Tri-planar – consisting of three planes.
- Trocar – a knife to create incisions in the sclera.
- Vitrectomy – removal of the vitreous fluid.